Improving Theranostic Proteins through PEGylation: Cancer-Imaging Antibodies

Honors Research Thesis

Presented in Partial Fulfillment of the Requirements for graduation "with Honors Research Distinction in Biochemistry" in the undergraduate colleges of The Ohio State University

By

Edward David Alten

Undergraduate Program in Biochemistry

The Ohio State University

May 2014

Thesis Committee:

Dr. Thomas Magliery, Advisor

Dr. Richard Swenson

Dr. Edward Martin Jr.

Abstract

Radioimmunoguided surgery (RIGS) utilizes radionuclide-labeled antibodies that bind to an epitope specific to certain cancers to detect and image tumors. The Magliery lab has developed a good RIGS candidate molecule called 3E8.scFv, which possesses many good theranostic properties but clears from the blood too quickly. Studies on the covalent attachment of polyethylene glycol molecules (PEGs) to proteins indicate that such PEGylation could improve certain theranostic properties in addition to increasing the clearance time.

Generally, however, the effects of PEGylation are poorly understood. My project is to study how PEGylation with different types of PEGs affects binding/activity, stability, size, and shape with the end-goal of improving 3E8.scFv as a RIGS molecule. I have studied PEG-conjugates of 3E8.scFv and 3E8cys.scFv (3E8.scFv with an added free cysteine) to characterize both the general behavior of PEGylated proteins and the differences between various types of PEGs.

We can get a preliminary analysis of the effects of PEGylation with SDS polyacrylamide gel electrophoresis (PAGE), but for more in-depth characterizations, we will use: surface plasmon resonance (SPR) to measure binding; gel filtration chromatography to measure size and aggregation; differential static light-scattering (DSLS) and differential scanning fluorimetry (DSF) to measure stability; and analytical

ultracentrifugation (AUC) and small-angle x-ray scattering (SAXS) to measure size/shape.

Currently, we can non-specifically PEGylate 3E8.scFv via N-hydroxysuccinimide (NHS)-ester chemistry at lysines and specifically PEGylate 3E8cys.scFv via maleimide chemistry at the added free cysteine. Both processes are verified via SDS-PAGE analysis. We have assessed the binding and stability of 3E8.scFv, 3E8cys.scFv, and various PEG-conjugates of each using SPR and DSF, which indicate little loss in binding or stability from a single PEGylation at the cysteine in 3E8cys.scFv or from a low level of PEGylation of 3E8.scFv. With extensive characterization of PEGylation, we could explain how PEGylation improves theranostic effectiveness and better utilize it to improve theranostic proteins like 3E8.scFv.

Acknowledgments

I would like to thank my advisor, Dr. Tom Magliery, for giving me the opportunity to work in his lab as an undergraduate researcher. Indeed, I want to thank everyone in the Magliery lab for making my research experience fun and rewarding. Specifically, Dr. Brandon Sullivan taught me almost everything I learned in lab and was extremely helpful and supportive throughout my time in lab. I cannot imagine a research experience without Brandon, and I am eternally grateful for his mentorship. I would also like to thank Kim Stephany, Nick Long, and Shubham Mangla for rounding out an awesome antibodies and interactions group and for making the lab a fun place. Lihua Nie helped me with the storage of PEGs, Dr. Kiran Doddapaneni helped with ion exchange, and Anusha Kumar helped with DSF, and they all deserve credit for my success in my research. Dr. Drew Dangel was supremely helpful and very accommodating during my work with SPR at the PMGF, a facility to which I also owe thanks. I would also like to thank Dr. Edward Martin for allowing me to get involved on the medical side of this project and for helping me get shadowing experience, as well as for serving on my defense committee. I would also like to thank Dr. Richard Swenson for serving on my defense committee. Finally, I owe much thanks to the Department of Chemistry and Biochemistry and to the College of Arts and Sciences for funding via various rewards, including the generous Undergraduate Research Scholarship I received my junior year.

Vita

June 2010……Loveland High School

May 2014……Candidate for B.S. in Biochemistry, The Ohio State University

Fields of Study

Major Field: Biochemistry

Minor Field: Linguistics

Table of Contents

List of Tables

List of Figures

Chapter 1: Introduction

1.1 Cancer and Radioimmunoguided Surgery (RIGS)

Cancer surgery is currently dominated by positron emission tomography (PET), computed tomography (CT) and similar scans, which identify cancerous tissue based on properties that cancerous tissue exhibits *more* than other tissue. For example, a PET scan shows areas of high metabolism by detecting where fluorodeoxyglucose (^{18}F) (FDG), a glucose analog, is metabolized fastest. Cancer fits this category as cancerous cells have higher metabolic rates than normal cells and thus digest more FDG, allowing the cancerous tissue to be identifiable over the background. The problem with this is that other tissues may also exhibit high glucose metabolism, such as the liver and the brain. This means that it is often difficult to tell the difference between cancerous tissue and healthy tissue that exhibits similar qualities. More importantly, however, the tumor signal to background ratio is not as favorable as it could be. It would be ideal if cancerous tissue could be differentiated from healthy tissue using a characteristic that *only* cancerous tissue exhibits, thereby eliminating background signal.

Dr. Edward Martin, a surgical oncologist at The Ohio State University's Wexner Medical Center, has helped to develop a type of diagnostic and surgical technology called radioimmunoguided surgery, or RIGS. This surgery system relies on the above principle: detecting cancer based on some characteristic completely unique to cancer. The idea

behind RIGS is to use some form of an antibody to target some characteristic of cancerous tissue. This antibody or antibody fragment is then radiolabeled with some radioisotope that is detectable and has a half-life appropriate to imaging or detection before, during, and after surgery. In this way, the surgery can be guided by a radiolabeled immunoglobulin molecule, hence the term radioimmunoguided surgery. The labeled antibody would be injected into the patient in order to either detect the cancer or to get a working image to guide the surgery. The end goal is to have a camera that can convert the signal from the radiolabeled antibodies to a visual depiction right in the operating room. A probe would also be utilized for quick determinations and confirmations. This RIGS method is superior to current cancer surgery technology because, in theory, it allows detection of cancer without having as much background. A better signal to background outcome will likely result in a higher percentage of negative margins, which could mean that the surgical cut is well away from the border of the tumor. (A positive margin means that the surgical cut intersects the tumor and a close margin means that the surgical cut is very close to the border of the tumor.) A negative margin in surgery is highly correlated with survival, as shown in Figure 1.

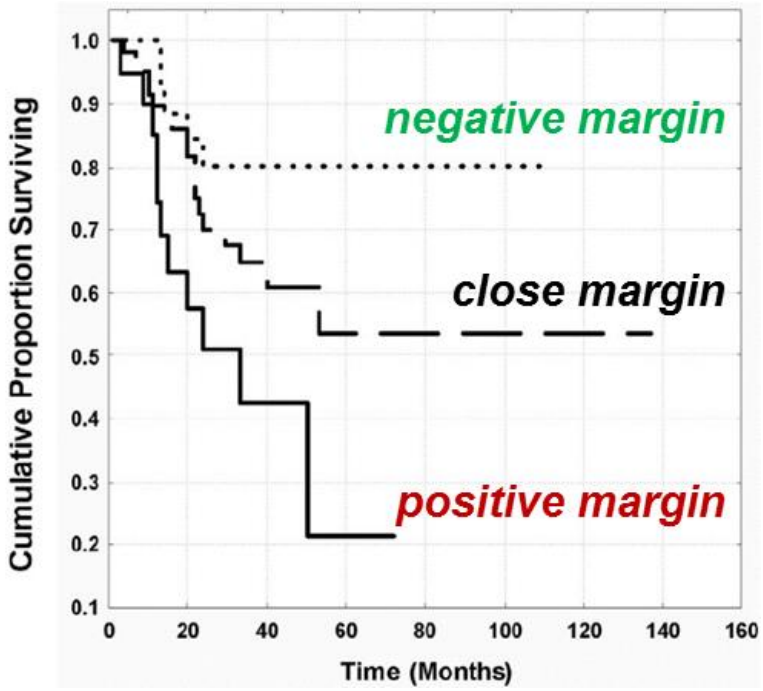

Figure 1. Surgical margins and survival[29]

Additionally, RIGS allows real-time imaging and detection during surgery, eliminating the often long wait times traditionally seen for obtaining a post-surgery scan to make sure the surgeon removed all of the cancerous tissue.[1-6]

1.2 Monoclonal Antibodies in RIGS

While a RIGS characteristic that applies to all cancerous tissue has yet to be discovered, there is a disaccharide called Sialyl-Tn that is part of a glycoprotein called tumor-associated glycoprotein 72, or TAG-72, in the mucin surrounding many types of cancers, especially adenocarcinomas.[7-9] A diagram of Sialyl-Tn and TAG-72 (labeled "mucin") is shown in Figure 2.

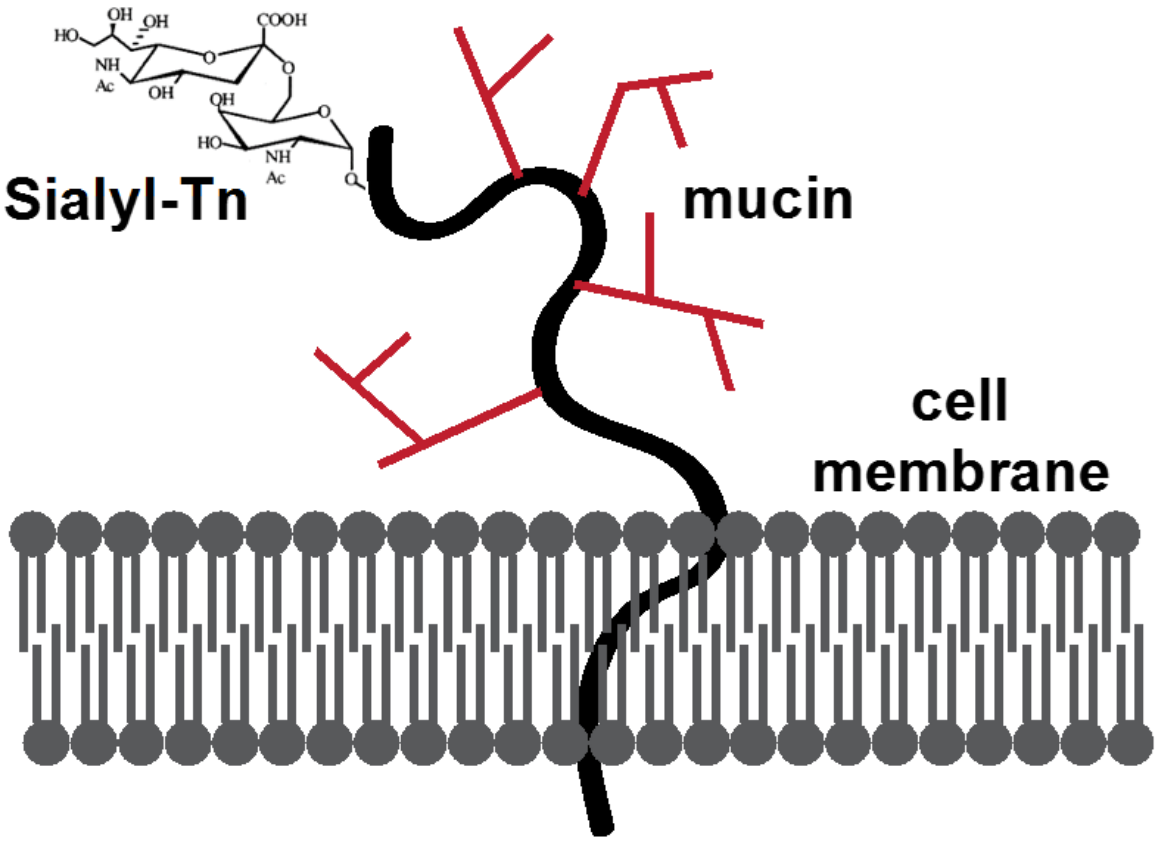

Figure 2. Diagram of Sialyl-Tn and TAG-72 in cell membrane

Monoclonal antibodies against Sialyl-Tn have been developed. The first such antibody was a full-length mouse antibody called B72.3.[8] This antibody, when moved into human trials, elicited the human anti-mouse antibodies response, or HAMA response.[10] The binding of B72.3 was improved in the next generation family of antibodies called CC49. However, CC49 still elicited the HAMA response, prompting a re-engineering of the scaffolding, resulting in a humanized version of CC49 called AKA.[11-14] Yoon et al. further advanced antibody design in this field by optimizing binding and then back-engineering AKA to a full-length antibody using human

scaffolding, resulting in a stronger-binding, more stable monoclonal antibody compatible with the RIGS system called 3E8.[15-17] A schematic describing antibodies and their fragments and showing the progression of TAG-72 monoclonal antibodies that have been developed for RIGS is shown in Figure 3.

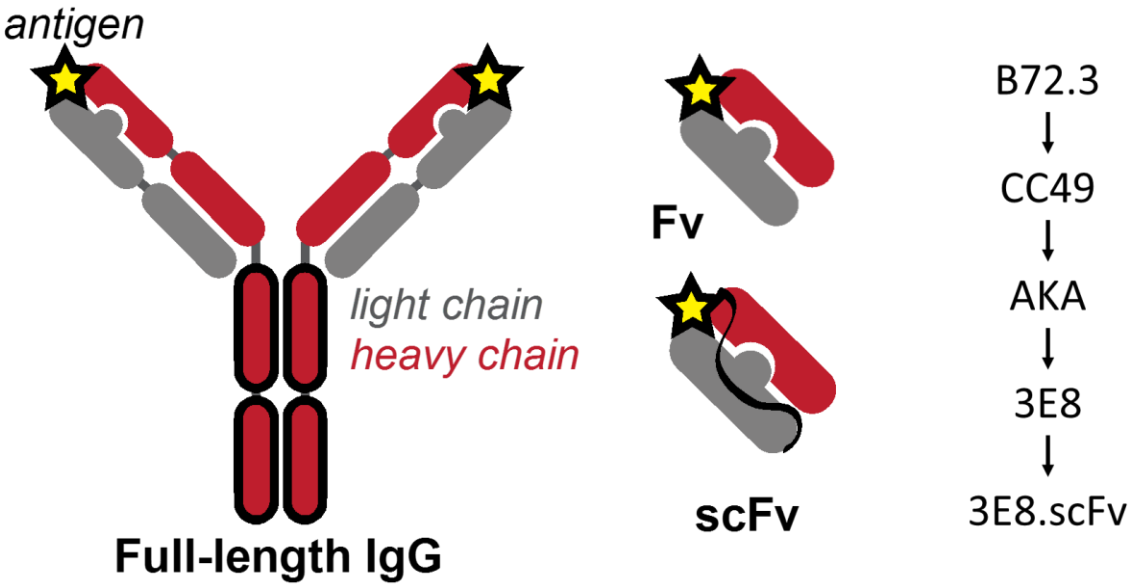

Figure 3. Antibodies and fragments and TAG-72 antibody progression

As hinted at in Figure 3, the Magliery lab took the full-length IgG 3E8 developed by Yoon et al. and engineered it into a single-chain variable fragment, or scFv. It is this molecule, 3E8.scFv, on which the work in this thesis is centered. 3E8.scFv is about 28 kD, composed of two chains, a variable heavy and a variable light chain linked together by a string of amino acids, resulting in a single protein that mimics the tip of the full-length IgG. The problem with 3E8.scFv lies in the fact that it is too small. When injected into mice, it is cleared by the kidneys and excreted too quickly to see significant exposure

to the cancerous tissue, which would allow it to bind and thus be used for detecting and imaging of the tumor. One way of making 3E8.scFv larger is by attaching a polyethylene glycol polymer, called a PEG. The problem with this is that, aside from a basic increase in size due to the added PEG, the exact effects of PEGylation, namely, structure function relationships, are not extensively studied, particularly in the case of antibody fragments. So, with the end goal of using 3E8.scFv as a RIGS theranostic molecule, PEGylation will be studied.

1.3 Polyethylene Glycol Polymers (PEG)

Polyethylene glycol (PEG) is a polymer with the general structure $H-(O-CH_2-CH_2)_n-OH$, shown in Figure 4.

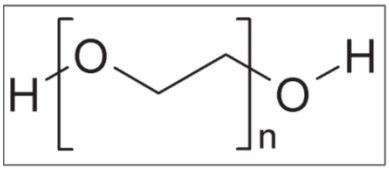

Figure 4. Basic structure of polyethylene glycol

PEGs can easily be created with various structures, meaning that its uses are myriad. There exist also many PEG derivatives that can be engineered for a host of applications. PEGs most commonly appear as the single, linear polymer of varying lengths. Recently, however, PEG derivatives that are branched, charged, and activated with various functional groups (for attachment to other molecules) are becoming more common. The classic production method is via polymerization, which is stopped at a

certain extent to create PEGs of a certain length. This creates PEGs that are referred to as polydisperse, meaning that the resulting mixture is not homogenous, but contains a mixture of PEG molecules of various, but similar lengths, with an average molecular weight. The degree of deviation from the average molecular weight can be characterized with something called the polydispersity index, which is the ratio of the average molecular weight of the mixture divided by the target molecular weight based on number of polymer units. Recently, production via polymerization has gotten more precise, resulting in much lower polydispersity indices.

Regardless, a company in Powell, Ohio, called Quanta BioDesign, has recently pioneered a different approach for producing PEGs. Quanta synthesizes PEGs and PEG derivatives from pure basic compounds via a series of step-wise reactions, producing discrete molecular weight compounds with specific structures and functional groups. Whether this accuracy in size is necessary or makes a difference in the various applications of PEGs remains to be seen.

PEGs are highly soluble in water and are non-immunogenic, meaning they do not elicit any immune response in human subjects. For these reasons, PEGs are commonly used to modify proteins and other molecules, especially in therapeutic and diagnostic (theranostic) roles.

1.4 PEGylation and Theranostic Proteins

The process of covalently attaching a PEG structure to another, usually larger molecule, like a protein, is referred to as PEGylation. (For simplicity, only the

PEGylation of proteins will be discussed here.) PEGylation to proteins can be accomplished using a variety of functional group and target residue pairs, especially NHS esters with lysine residues and maleimides with cysteine residues. These functional groups are attached to the PEGs during production and, usually, using a simple reaction setup, can be used to attach their PEGs to the target protein. The chemical reaction between an NHS-ester activated PEG and an amine, like a lysine, is shown in Figure 5. The corresponding chemical reaction between a maleimide activated PEG and a thiol, like a cysteine, is shown in Figure 6.

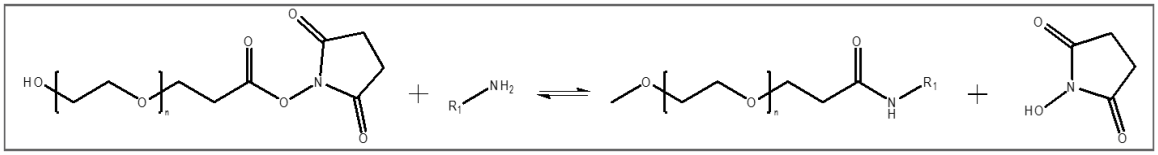

Figure 5. Reaction between an NHS-ester and an amine (Lys)

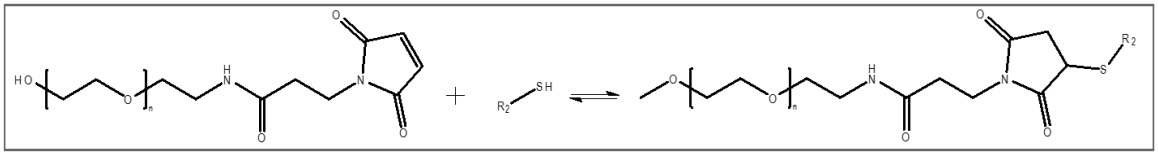

Figure 6. Reaction between a maleimide and a thiol (Cys)

A question that remains to be answered regarding the PEGylated product is how the PEG behaves once attached. It is possible that the PEG could wrap around the protein like a rope, but more likely, the PEG would behave according to polymer theory, forming a spherical blob near the attachment point. In either case, the potential benefit of

attaching the PEG derives from its modification of the size, shape, and solubility of the protein being modified.

There are commonly proteolytic and immunogenic sites present on the solvent-exposed portions of proteins, so if these proteins are to be used theranostically, these sites must either be engineered out or covered up. PEGs can do the latter, effectively eliminating sites where proteases might have otherwise cleaved the target protein and sites where elements of the human immune system might have recognized the protein as being foreign. Additionally, if a protein has solubility issues, adding a PEG, which is extremely soluble, could increase the solubility of said protein. One of the most important modifications PEGylation can create is in size. Filtration by the kidneys is largely based on size, so the time a potential theranostic protein spends in the blood, measured via serum half-life, can be affected by changing its size, in this case by attaching PEGs. Another factor important to kidney filtration is shape. PEGylation obviously affects this as well, and, as discussed before, the shape of PEGylated proteins is not immediately obvious. If the PEG wraps around the protein, its shape will remain similar to that of a single sphere; but if the PEG forms its own sphere near its attachment point, the shape of the protein is wildly changed as it is now more like a peanut, with two spheres next to each other.[18-21]

1.5 Studying PEGylated Proteins

Largely, the aim of my research is to study the biophysical effects of PEGylating a protein. Obviously, to do this, various assays and techniques will be utilized. Many of

these are very simple and/or very common. Some, however, require some explanation. In order to measure the binding of a protein (in this case, an antibody fragment – but more on that later), a technique called surface plasmon resonance, or SPR, will be used. In this experiment, a ligand is bound with NHS-activation chemistry to a gold chip derivatized with dextran. A beam of light is focused onto the chip from the other side and has a certain angle of reflection. The target protein which binds to said ligand is then flowed over the chip at a constant rate. When the protein binds to the ligands bound to the chip, the angle of reflection of the light beam changes and this change is detected. The more protein that binds to the ligands bound to the chip, the greater the change of the angle of reflected light. In this way, the rate of association (the rate at which the protein binds to its ligand) can be measured using a program that fits the resulting curve to an equation. When nearing saturation, the protein ceases to be flowed over the chip, being replaced with a blank solution containing no protein. This allows the proteins already bound to the ligands on the chip to unbind, or dissociate. The angle of reflection changes again as protein dissociates, allowing the rate of dissociation to be measured as well. Using this association and dissociation data, the binding constant for the protein can be calculated.

In order to determine the shape via hydrodynamic radius, analytical ultracentrifugation, or AUC, can be used. In this technique, a solution containing a molecule of interest is centrifuged at high speed into a medium and the sedimentation is measured and can be equated to various aspects of the molecules size and shape.

Chapter 2: Objectives

2.1 Expression and Purification of Proteins (3E8.scFv and 3E8cys.scFv)

In order to study PEGylation and how it might apply to RIGS, it would be convenient to use the actual molecule that will be utilized in the RIGS system, if the long-run goals are met. This way, the results of a rigorous study of PEGylation would overlap with the application of such PEGylation to the specific problem at hand, namely, to modifying the pharmacokinetic properties of an antibody fragment being used to detect and image cancer. Therefore, the expression and purification of both the actual protein being used (3E8.scFv) and of a version slightly modified to make PEGylation studies simpler (3E8cys.scFv), should be optimized to yield an acceptably high amount of active protein.

2.2 Nonspecific PEGylation at Lysines and Characterization

Studying PEGylation via nonspecific modification using NHS-ester chemistry at multiple lysines is a good place to start because it is inexpensive and can be done on most proteins without modification. (This compared to specific PEGylation with maleimide chemistry, which requires free cysteines, a relatively rarer feature of proteins.) By nonspecifically PEGylating at lysines, the PEGylation procedure can be optimized and the general effects of PEGylation, particularly on stability and activity, can be observed

via various assays and experiments. There are confounding issues in these experiments, however, in that specific lysines might cause more problems than others.

2.3 Specific PEGylation at Cysteines and Characterization

To more accurately characterize the effects of PEGylation, single PEGylation events must be isolated and studied in full before expanding to generalization about multiple PEGylation events, as in objective 2. Using specific and single PEGylation, comparisons between different types and sizes of PEGs can be made, specifically between 5, 20, and 40 kD PEGs, and between a linear and a Y-shaped branched PEG. These comparisons will hopefully shed some light on the structure-function relationships of PEGs and PEGylated protein conjugates.

Chapter 3: Methods

3.1 Expression and Purification of Proteins (3E8.scFv and 3E8cys.scFv)

Cytoplasmic Purification

The following expression/purification scheme is a modified version of a standard *E. coli* expression and immobilized metal ion affinity chromatography (IMAC) purification protocol.[22] Following the same protocol for each, the following proteins were overexpressed in BL21(DE3) *E. coli* cells, unless stated otherwise: T4L, CC49, CC49.cyto (lacks a Pel-B leader sequence), 3E8.scFv, and 3E8cys.scFv. The genes for these proteins were in pCOLD or pHLIC, and during optimization, the *E. coli* strain was varied to C41(DE3), C43(DE3), NEB Xpress, DH10B(DE3), etc. Small 25 mL overnight cultures picked from colonies plated after transformation the day before were used as seeds for larger liquid cultures. These larger cultures were generally grown in 4 L non-baffled flasks, containing 2 L of 2YT media, at 37 °C and shaken at 100-125 rpm (or 200 rpm for T4L). For all proteins except T4L (for which this step was skipped), the flasks were then cold-shocked at log phase, or $OD_{600} \approx 0.75$. This was accomplished either by swirling them in an ice bath or by letting them sit in the cold room at 4 °C (or both) for 10-20 min. Then, the cultures were induced with IPTG to 0.05 mM (0.1 mM for T4L) and were kept at 4 °C for an additional 10-15 min. They were then allowed to continue growing overnight at 16 °C (T4L was grown for another 3 h at 37 °C).

The cells were then centrifuged at 4 °C and 6000 rpm for 5 min and the pellets (sometimes frozen at -80 °C or -20 °C first, for storage) were resuspended in 20-25 mL lysis buffer (50 mM Tris-HCl, 300 mM NaCl, 10 mM imidazole, pH 8) per liter of culture represented in the pellet. The resuspended cells were then mixed with 5mM $MgCl_2$, 0.5 mM $CaCl_2$, 5 µL of both DNase I and RNase A (at 5 mg/mL each) (per liter of culture represented), 0.1% Triton X-100, and 10-30 mg of HEW lysozyme (per liter of culture represented). This mixture was then allowed to incubate on ice/at 4 °C for at least 30 min with agitation every 5 min or constant mixing via the mutator. The cells were then lysed with one or a combination of several methods: sonication, glass beads, and Emulsiflex. Sonication was performed at amplitude 7 by pulsing the resuspended pellet 4 times at 30 sec each with 2 min breaks between pulses. The glass bead method was performed by adding about 0.5 mL of 0.1 mm glass beads (per liter of culture represented) to the resuspended pellet mixed with the lysing ingredients (as above) and vortexing for 3 min, 30 seconds at a time with 3 min on ice between pulses. The Emulsiflex was used to lyse cells by cycling the sample through the machine three times at a pressure differential of between 15,000 and 20,000 psi, keeping it on ice between cycles.

The lysate, once homogenous, was centrifuged at 4 °C and 15,000 rpm for 1 h. The supernatant was allowed to bind to 1 mL Ni-NTA agarose resin (Qiagen) per liter of culture for at least 30 min at 4 °C on the mutator. The mixture was then poured into a column (larger size, 20 mL), washed with wash buffer (20 mM imidazole), and eluted with elution buffer (250 mM imidazole). Between a 0.04 and 0.08 mg of TEV protease

was added to the elution twice; the first time, allowed to incubate overnight at room temperature and the second time, in the morning before continuing with the purification a few hours later, both times with 1 mM DTT. The resulting cleaved solution was desalted using a PD-10 column (GE Amersham) and swapped into TIM Storage Buffer (300 mM NaCl, 100 mM phosphate, pH 7.4) or lysis buffer. The buffer-swapped solution was then bound to 0.5 mL Ni-NTA per liter of culture the same as the first step. Another column was run (smaller size, 10 mL) and the flow-through was collected and kept as the cleaved, purified protein. The column was also washed with lysis buffer and/or dilutions of wash buffer and eluted with elution buffer. The flow-through was concentrated using Amicon Ultra 10,000 MWCO (Millipore) Centrifugal Filters and/or swapped into PBS buffer via dialysis (10,000 MWCO snakeskin or cassettes) as necessary.

Periplasmic Purification and Modifications

This purification method was used on CC49.cyto (lacks a Pel-B leader sequence) and 3E8.scFv. It is identical to the normal cytoplasmic purification (above) up to the point of resuspending the pellets. Instead, the pellets in this method (Protocol 11. Preparation of 6xHis-tagged periplasmic proteins from *E. coli*, published by Qiagen) were resuspended in a buffer containing 30 mM Tris·HCl and 20% sucrose at pH 8.0 at a ratio of 80 mL per gram of wet weight in the pellet. Then, 500 mM EDTA was added incrementally, on ice. This mixture was then incubated on the mutator for 30 min and then centrifuged at 4 °C and 8,000 g for 20 min. The supernatant was decanted and saved (sucrose step) and the pellet was resuspended in the same volume of cold 5 mM $MgSO_4$

and incubated on the mutator at 4 °C for 30 min. The mixture was again centrifuged the same as before and the supernatant was saved ($MgSO_4$ step). The sucrose and the $MgSO_4$ steps supernatants were concentrated and then dialyzed into lysis buffer using cassettes. The purification then proceeded as above (Ni-NTA and column) but was stopped after the first column to assess yield.

Multiple modifications were made to this procedure to optimize yield. Certain things about the procedure were changed individually: EDTA was not added in one version, no dialysis was performed in another, and instead of relying on only osmotic shock to lyse the outer membrane, lysozyme was also employed in one version, which was further split into two experiments in which the osmotic shock was conducted before or after the first centrifugation step.

3.2 Methods for Nonspecific PEGylation at Lysines and Characterization

PEGylation at Lysines

Various PEGs with NHS-ester functional groups were stored at -20 °C in a tube/container with Drierite and were allowed to come to room temperature before being opened. The PEGylation procedure used was based on a procedure published by Thermo Scientific for PEGylating Proteins using NHS-PEGylation. Before the reaction takes place, the sample to be PEGylated should be dialyzed into PBS to avoid NHS-Tris reactions. A PEG stock solution of a certain concentration (calculated according to needs) was created by dissolving the appropriate amount of PEG in DMF. The appropriate amount of this stock solution to obtain the desired molar excess of PEG to protein was

then mixed with the protein solution (in PBS), being careful to keep the total amount of PEG solution under 10%, and preferably under 5%, if possible. The reason for this was that PEG was treated as potentially damaging to the protein's fold at high concentrations. The total reaction volume was kept the same so the final concentration of the protein in every reaction remained constant. The reaction mixture was then mixed via vortexing and allowed to react at room temperature for 30 min-2 h depending on the desired extent of PEGylation. The reaction was then quenched with 100x excess (to the amount of PEG) of ethanolamine.

EnzChek® Lysozyme Assay Kit

The EnzChek® Lysozyme Assay Kit by Molecular Probes (sold by Life Technologies) was used with T4L to assess activity after PEGylation to various degrees. The procedure laid out in the kit was followed very closely. First, a standard curve was produced by making lysozyme substrate and standard lysozyme (both included in the kit) stock solutions of 1.0 mg/mL and 1000 U/mL respectively in 1.0 mL deionized water each. The experimental samples of PEGylated lysozyme (T4L, produced following the cytoplasmic purification in objective 1, and PEGylated at various molar excesses according to the PEGylation procedure in objective 2) were diluted using the included reaction buffer (50 mL of 0.1 M sodium phosphate, 0.1 M NaCl, pH 7.5, and 2 mM sodium azide as a preservative). The standard lysozyme was serially diluted into 8 wells with the included reaction buffer. The stock substrate solution was diluted further to create a working substrate solution, which was then added to each of the wells containing

either standard or experimental lysozyme solutions. The plate containing the reaction mixtures was then incubated in the fluorescence microplate reader for 30 min at 37 °C while the reader took fluorescence readings with standard fluorescein filters for absorption maxima at 494 nm and fluorescence emission maxima at 518 nm. The background fluorescence was then subtracted out.

Glycol Chitosan and the Imoto Assay

An alternative to the EnzChek® assay was discovered in da Silva Freitas' paper[23] but was originally published in 1971 by Imoto and Yagishita.[24] It assays lysozyme activity using the substrate glycol chitosan. It is performed my mixing 1 mL of 0.05% glycol chitosan in 100 mM pH 5.5 acetate buffer with 100 µL of lysozyme/modified lysozyme solution and incubating the mixture at 40 °C for 30 min. Then, 2 mL of the color reagent ($[Fe(CN)6]^{3-}$ dissolved in 0.5 M Na_2CO_3) was added and the mixture was boiled for 15 min. After cooling, the absorbance was read at 420 nm in a fluorimeter.

Differential Scanning Fluorimetry (DSF)[25]

The PEGylated protein samples were mixed (19 µL) with 1 µL of the diluted SYPRO® Orange dye (Invitrogen) (provided as 5000x, diluted to 300x before addition, and then to 15x in the final mixture) in 96-well 0.2 mL thin-wall PCR plates (USA Scientific), sealed with Adhesive PCR Film (Thermo Scientific). Using a BioRad C1000 Thermal Cycler, the temperature was increased by 0.2 °C every 12 s to acquire thermal denaturation curves, with the fluorescence intensities measured using a 490 ± 10 nm

excitation filter (from the SYBR Green set) and a 575 ± 10 nm emission filter (from the FRET filter set). Data were exported and analyzed in Microsoft Excel 2010/2013.

Surface Plasmon Resonance (SPR)

The SPR performed was based on the literature for CC49.[26,27] A CM5 chip was used in a Biacore T100. Scouting determined that 100 mM NaAc, pH 4 was a good immobilization buffer. BSM (positive for the Sialyl-Tn ligand) at 0.5 mg/mL and BSA (negative control) at 0.016 mg/mL were immobilized using the Amine Coupling kit (Pharmacia Biosensor), using N-ethyl-N-(3-diethylaminopropyl) carbodiimide (EDC) and NHS, quenching with ethanolamine/HCl (pH 8.5) and washing with 50 mM NaOH, until a surface of 700 resonance units was obtained, as per Pavlinkova *et al*.[27] Then, binding analyses were performed in (HBS) buffer (10 mM (N-[2-hydroxyethyl]piperazine-N'-[2-ethane sulfonic acid]) [HEPES] [pH 7.4], 0.15 M NaCl, 3.4 µM EDTA, 0.005% surfactant P20) using the following parameters: samples were flowed over the chip for a contact time of 120 s, a flow-rate of 10 µL/min, and a dissociation time of 180 s; then the chip was regenerated with 6 M guanidine, 200 mM HOAc buffer with a 30 s contact time at a flow rate of 30 µL/min and a 0 s stabilization time. The range of concentrations used spanned from 5 nM to 400 nM, but the final set of concentrations that yielded the best results was 0, 5, 10, 25, 50, 75 (duplicate), 100, 150, and 200 nM. This range is suggested by the programming of the protocol on the software and is used to get a more accurate evaluation by taking into account the binding behavior at multiple concentrations. Once all the concentrations were run, the curves were fit using

the kinetics 1:1 global fit, over the whole series of concentrations, but changing the R_{max} fit to local instead of global on the BIAevaluation 3.0 software (Biacore, Inc.) where the experimental design correlated with the Langmuir 1:1 interaction model.[28] This yielded a k_a, a k_d, and from those, a K_D. The R_{max} values were also recorded for proper comparison.

Circular Dichroism[22]

Data were collected on a Jasco J-815 CD spectrometer. TIM samples were diluted to 12 μM in 50 mM potassium phosphate and 300 mM NaCl, pH 8. Far-UV spectra were recorded in triplicate from 195 to 250 nm. Wavelength scans recorded ellipticity every nanometer with 2-s integration time and 100 $nm \cdot min^{-1}$ scanning speed. Data points reporting HT voltages greater than 600 V were discarded. For thermal denaturation, ellipticity was monitored at 222 nm with temperatures increasing from 25 to 95 °C. Data were collected in 1 °C steps with 6-s temperature equilibration, 1 °C min−1 ramping and 2-s integration. Data were exported and analyzed in Microsoft Excel 2010/2013.

3.3 Specific PEGylation at Cysteines and Characterization

PEGylation at Cysteines

Specific PEGylation at cysteines using maleimide chemistry is performed similarly to nonspecific PEGylation at lysines using NHS-ester chemistry, described above, in objective 2 methods. Maleimide is not as liable to hydrolysis, however, so DMF does not need to be used: instead, the PEG stock solutions are made using PBS buffer. Again, the total volume of the reactions is kept the same so that the final concentration of

protein is the same for the various molar excesses and different PEGs. The reactions here take place overnight at room temperature and do not require quenching. Because the PEGs being used here were so much larger than the PEGs used for objective 2, the PEG stock solution, even though it contained no DMF, was still considered to be slightly organic because PEG is amphiphilic, and so was added in increments to the protein solution instead of all at once.

Ion Exchange

An ÄKTApurifier 900-series FPLC using a 1 mL RESOURCE™ S column (GE Healthcare) was used for ion exchange. The low salt buffer used was 50 mM potassium acetate, 15 mM sodium chloride, pH 5 (buffer A) and the high salt buffer used was 50 mM potassium acetate, 1 M sodium chloride, pH 5 (buffer B). A 1 mL loop was used and initially, a 200 column volume (CV) gradient (from 15 mM to 1 M NaCl) was set. During the runs, the flow rate was increased as long as the pressure limit was not exceeded. In addition, if it appeared that protein was not eluting (via a flat UV signal, between peaks), the gradient length was decreased to 20 CV to speed up the process. This was monitored very carefully and immediately increased back to 200 CV if anything appeared to be coming off the column (a rise in UV signal).

Gel Filtration

The buffer used for gel filtration was 50 mM Tris, 100 mM NaCl, pH 8.0. The same FPLC used for ion exchange was also used here, but the column used was a 25 mL

Superdex™75 10/300 GL column (GE Healthcare). In this experiment, a 200 µL loop was used.

Chapter 4: Results and Discussion

4.1 Expression and Purification of Proteins (3E8.scFv and 3E8cys.scFv)

Figure 7 shows an SDS PAGE Gel of a purification of T4L. FT2 and W2 are the final, purified protein in a high concentration. After TEV cleavage and a second Ni-NTA column, T4L is shown to be purified in high purity. It appears, however, that there could be a small molecular weight contaminant at the dye front. Consequently, if this was to be used for sensitive studies, further purification might have been needed.

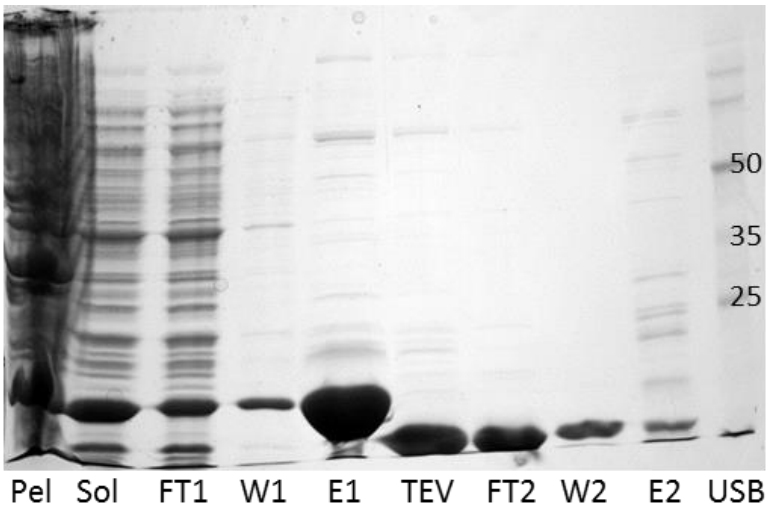

Figure 7. Gel of purification of T4L

This protein was later used for nonspecific PEGylation experiments because of its 13 surface lysines and one surface cysteine, shown in Figure 8, which also depicts the active site of T4L.

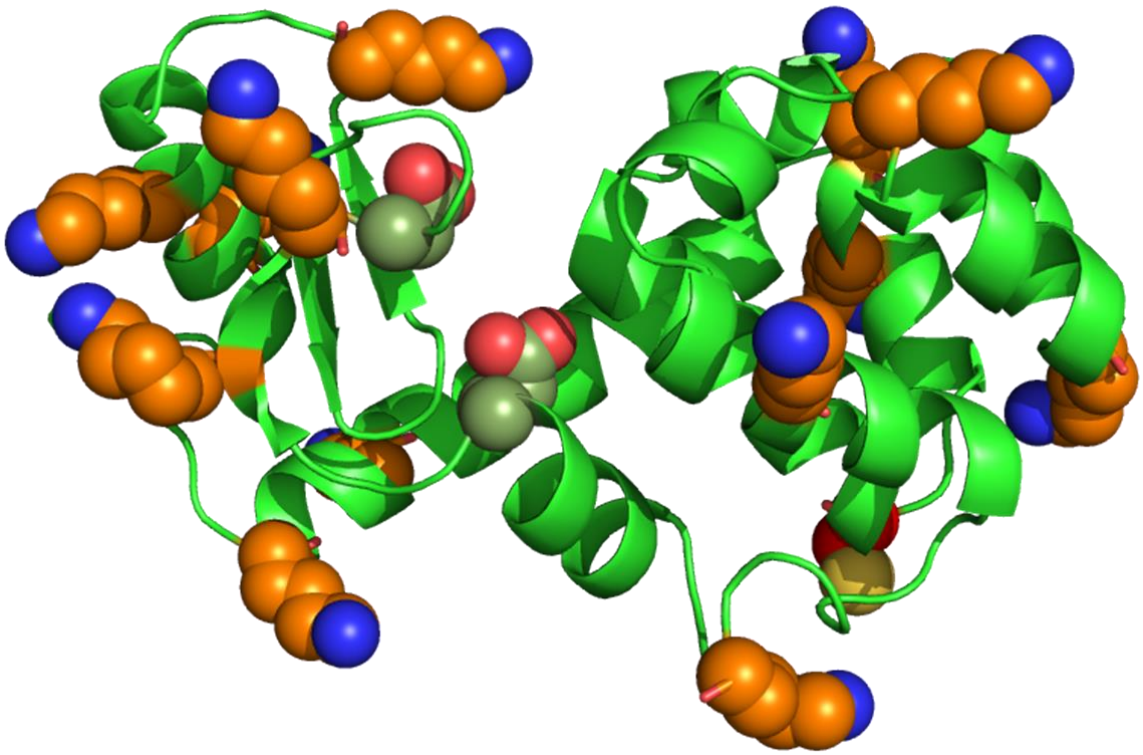

Figure 8. T4L with orange/blue Lys, yellow/red Cys, and grey-green\red active site

Later, we had trouble reproducibly expression T4L, so we stopped using it in favor of the actual 3E8.scFv or 3E8cys.scFv for PEGylation experiments.

As described in the methods section, multiple modifications were made to the periplasmic purification method published by Qiagen. These modifications are described in Figure 9.

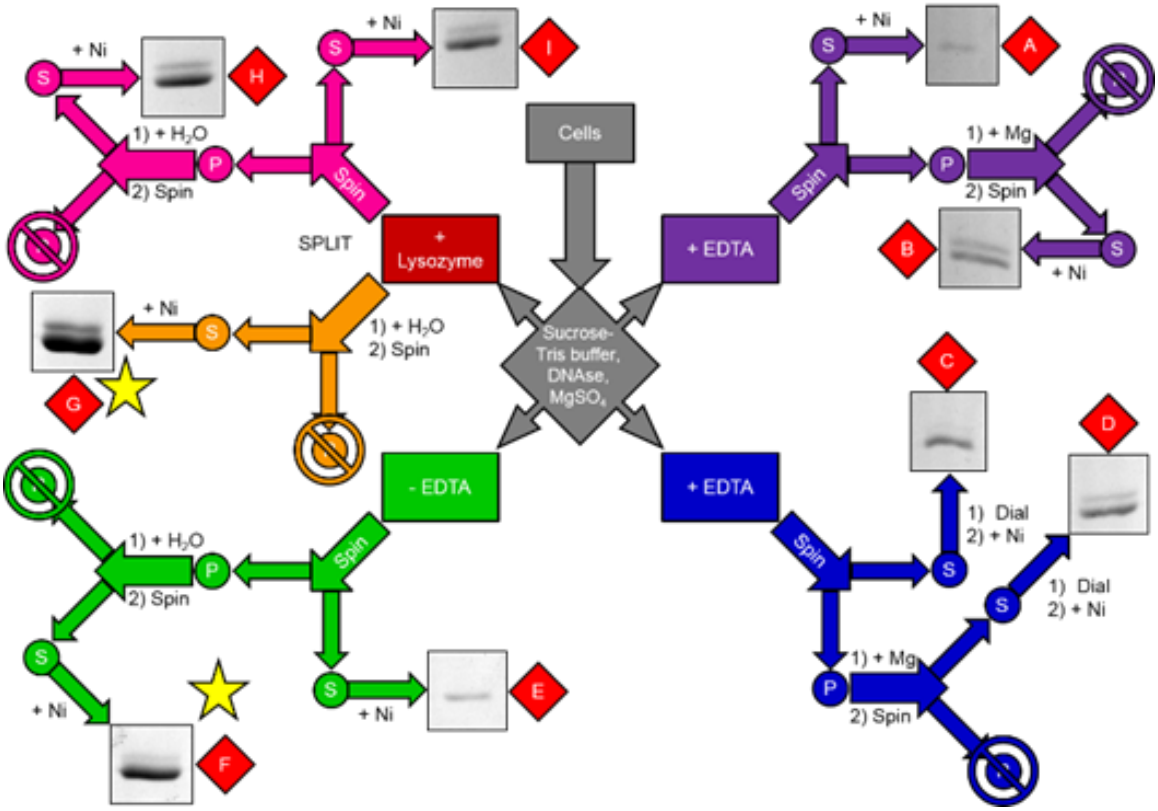

Figure 9. Periplasmic purification of 3E8.scFv: modifications and results

Figure 9 shows a number of modifications. The original periplasmic purification procedure published by Qiagen is represented by the blue boxes and arrows, and the results of that purification are shown in C and D. The dialysis step in this procedure was removed and this procedure is represented by the purple boxes and arrows, with the results shown in A and B. This modification resulted in less purified protein after the first Ni-NTA column, likely because the EDTA was not removed by dialysis, thereby allowing it to chelate some of the nickel in the Ni-NTA resin. Then, the EDTA was removed from the procedure all together along with the dialysis step, which was only there to remove the EDTA. Additionally, the 5 mM $MgSO_4$ was only there to attempt to

sequester the EDTA, so with the EDTA removed, the $MgSO_4$ was also removed. This procedure is represented by the green boxes and arrows, with the results shown in E and F. This was the best modification yet. The EDTA was originally used because it was thought to disrupt the membrane by sequestering calcium associated with the membrane. The membrane being disrupted meant that when the osmotic shock was performed, it would be easier for the protein of interest to exit the membrane. Evidently, EDTA was not necessary and in fact appears to have been detrimental to the purification. Instead of using EDTA to disrupt the outer membrane, then, (hen egg white) lysozyme was used, shown in the red box. This procedure was then split again, and in one branch, represented by the orange boxes and arrows, the osmotic shock was performed right away, followed by the rest of the procedure as normal. This resulted in the product labeled G, which was the most protein produced by any purification yet. Finally, the second branch using lysozyme to disrupt the membrane is represented in the red boxes and arrows, with the results labeled H and I. This procedure was similar to the orange procedure, but the original centrifugation step was added back in directly after letting the cells incubate in lysozyme. This was removed in the previous orange branch because it was thought – and confirmed – that any protein that had leaked out after disruption of the membrane would simply stay in solution after the osmotic shock and resulting spin. This is evidenced by the fact that it looks as if the product labeled G is about the same amount of protein in the products of H and I combined. Therefore, the "G" procedure was the "optimized" periplasmic purification procedure that was used until a better method – pHLIC in C43, lysis method – was discovered later.

At this point, 3E8.scFv in pCOLD was being produced in BL21(DE3). The results of the various modifications are shown in Figure 9 and the modifications that produced the most protein, labeled F, G, H, and I, were further examined by conducting the TEV reaction as described in the methods, the results of which are shown in Figure 10.

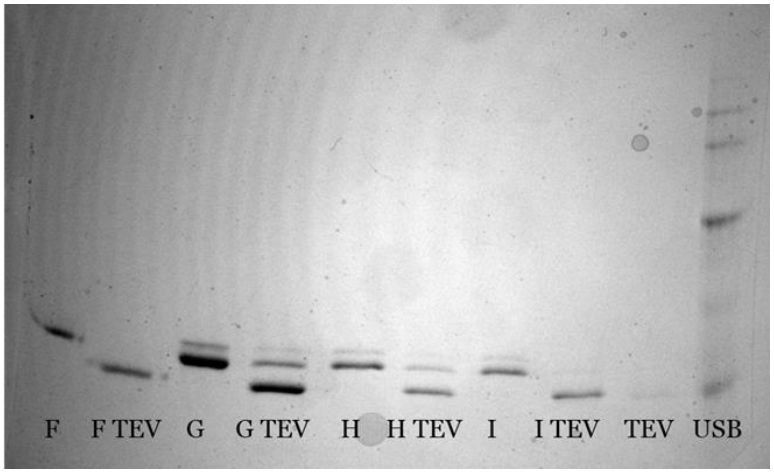

Figure 10. TEV cleavage of most promising samples from Figure 9

The final purification modification that was used to produce 3E8.scFv was the one labeled G, which followed the Qiagen method but did not add EDTA, instead adding hen egg white (HEW) lysozyme, before performing osmotic shock with water (instead of 5 mM $MgSO_4$). The rest of the purification was conducted the same way as the normal purification protocol described in methods. This "G" method was the preferred purification/expression scheme until different strains were tested and it was discovered that a similar amount of protein could be produced using the C43(DE3) strain with the gene in the pHLIC plasmid.

Several other strains apart from BL21(DE3) were tested to see if the pCOLD plasmid could produce protein more effectively. Figure 11 shows the result of using DH10B(DE3) and NEB Express (New England BioLabs) *E. coli* cells with the original pCOLD plasmid and both 3E8.scFv and 3E8cys.scFv. Neither strain produced either protein any more efficiently than the BL21(DE3) cells did.

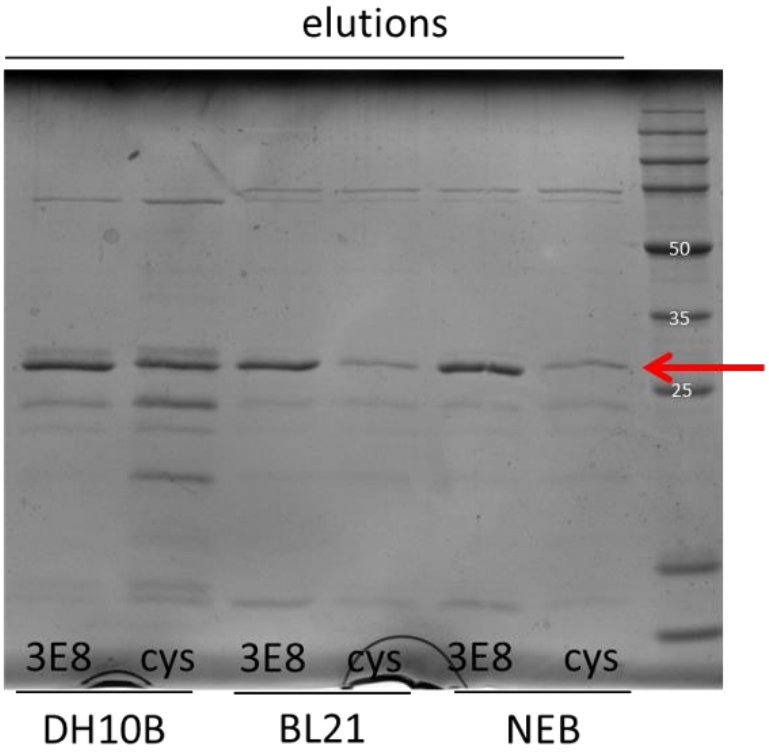

Figure 11. Three E. coli strains' production of 3E8.scFv and 3E8cys.scFv

At this point, the genes for 3E8.scFv and for 3E8cys.scFv were swapped into the pHLIC plasmid from the pCOLD plasmid and the C43(DE3) cell line was used to once again attempt to optimize production. Figure 12 shows the results of using C43(DE3)

cells to produce both 3E8.scFv and 3E8cys.scFv from the pHLIC plasmid. This combination of plasmid and cell line resulted in the best yield of either protein up to that point, and it was done via the cold shock method, but using the original complete cell lysis method, not the optimized osmotic shock method previously referred to as the "G" method. This purification scheme was then adopted for producing all 3E8.scFv and 3E8cys.scFv.

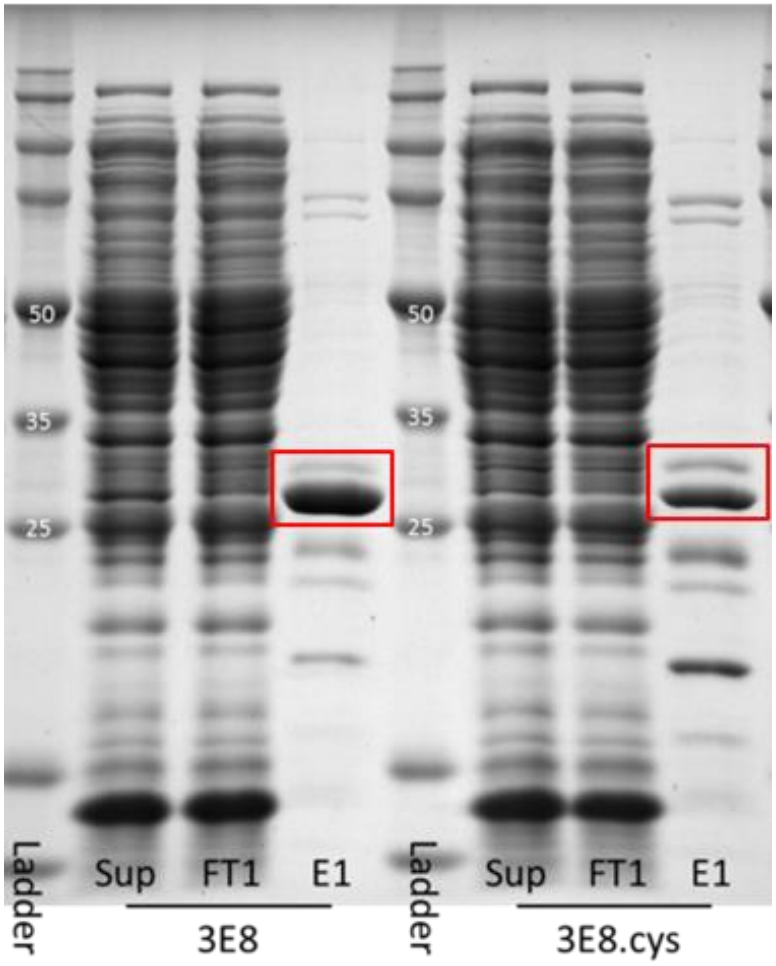

Figure 12. Expression of 3E8 fragments using pHLIC and C43 cells

4.2 Nonspecific PEGylation at Lysines and Characterization

The first attempt at nonspecific PEGylation at lysines using NHS-ester activated PEGs is shown in Figure 13. In this experiment, T4L was PEGylated with a 2 kD polydisperse NHS-ester PEG (Creative PEGWorks). The result of reactions using various molar excesses of PEG to T4L are shown. At lower excesses, bands above the band representing unPEGylated T4L start to appear in a stepwise fashion. These represent T4L molecules with integer numbers of PEGs attached. It can be seen that at higher excesses, the ladder of PEGylation products on the gel blend into a continuous smear. This could have something to do with large amounts of DMF or it could be a result of large amount of PEG binding to SDS at different charge-to-mass rations, resulting in a smear.

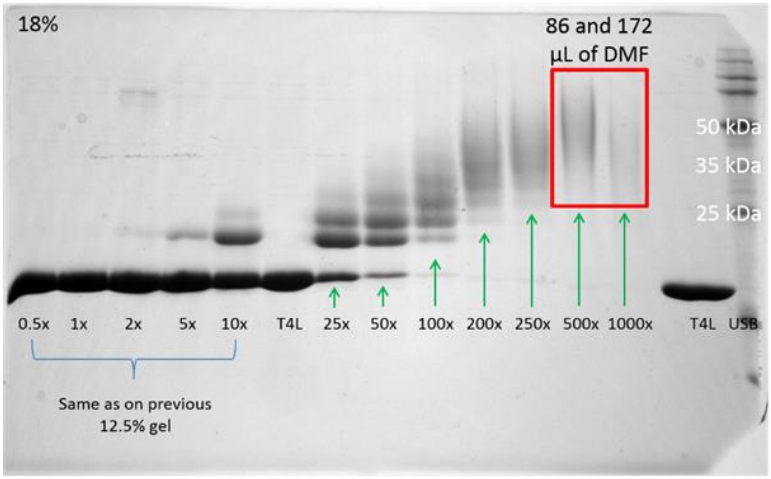

Figure 13. Nonspecific PEGylation of T4L with polydisperse 2 kD NHS-ester PEG

This experiment was repeated (except with fewer molar excesses) in parallel with a very similar experiment, which used 1.8 kD discrete NHS-ester PEG (Quanta

BioDesign) instead of the 2 kD polydisperse PEG. Figure 14 shows the results of this experiment: a smear of bands on the left side (polydisperse PEG) like those that were seen in Figure 13, but a clear ladder of bands on the right side (discrete PEGs). This is likely due to the nature of polydisperse and discrete PEGs: the former are of an average size but have variation in the size of individual molecules, while the latter are all exactly the same molecular weight.

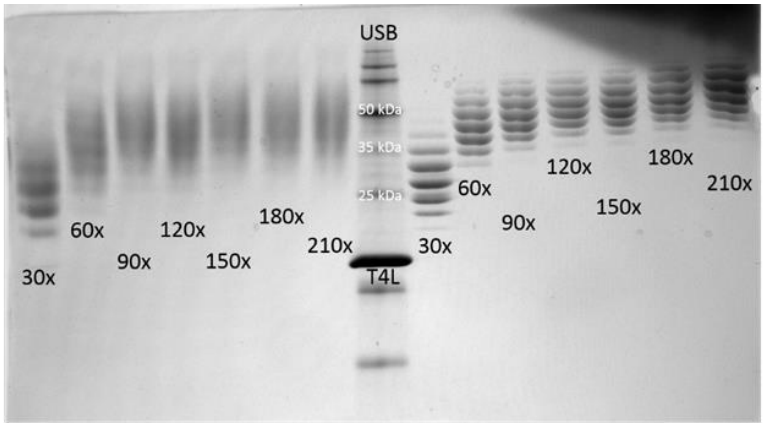

Figure 14. Nonspecific PEGylation of T4L with 2 kD PEGs

Figure 15 shows the results of a repeat of the above experiment, PEGylating T4L with the same 1.8 kD discrete PEG (Quanta BioDesign), but at a wider range of molar excesses. (This was also repeated with the 2 kD polydisperse PEG as well, but the gel is not shown). It is indicated that a total of 14 bands above the unPEGylated T4L can be seen on the gel; there are 13 lysines in T4L, so the 14th band up represents T4L in which all 13 lysines and the amine group at the N-terminus are all PEGylated.

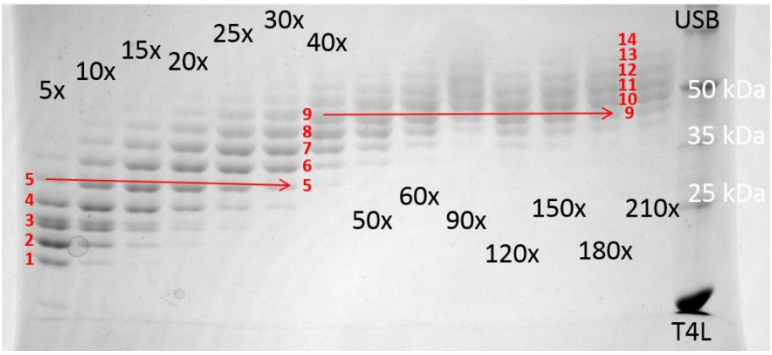

Figure 15. Nonspecific PEGylation of T4L with discrete 1.8 kD NHS-ester PEG

The samples shown in Figure 15 and discussed above, as well as the parallel samples PEGylated with the 2 kD polydisperse PEG, were characterized a variety of ways. The first, shown in Figure 16, was using the EnzChek® Lysozyme Assay Kit. Displayed as a bar graph, the fluorescence of each of the PEGylated T4L samples is shown and should be compared to that of the unPEGylated T4L sample, on the far right.

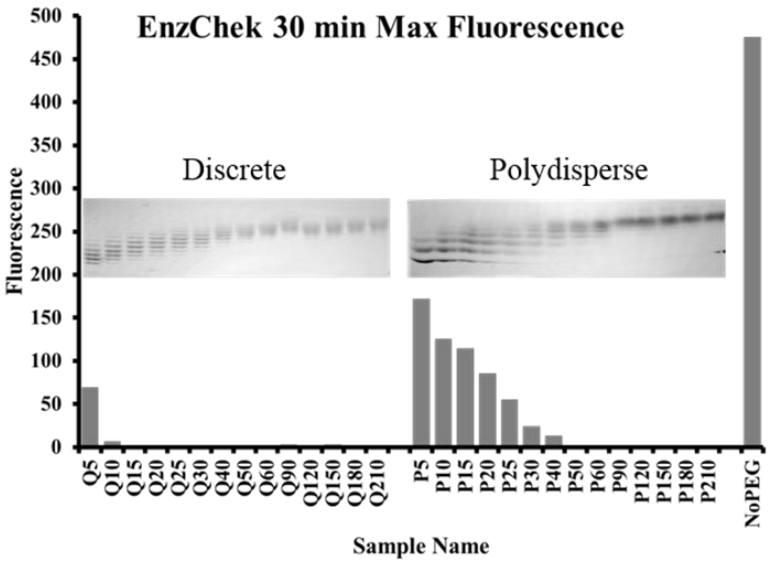

Figure 16. EnzChek® assay showing relative activities of PEGylated T4L

In this assay, fluorescence is proportional to activity. Somewhat predictably, the unPEGylated enzyme is the most active. Less predictable, however, is the nearly complete lack of fluorescence, and thus activity, of most of the PEGylated samples, particularly of the samples PEGylated with the discrete PEG. There is a general trend of less activity with greater molar excesses in the PEGylation reactions, i.e., with more attached PEGs per molecule. There are two immediately obvious explanations for this: either higher loads of PEGs ablate activity in general (either by unfolding the protein or by blocking the active site), or there are one or more specific lysines that, when PEGylated, result in a complete loss of activity. These two explanations are indecipherable using current data but this questions is being pursued by another undergraduate student in the Magliery Lab. If the latter is the case, then the level of fluorescence seen would correlate to the amount of unPEGylated T4L seen in each sample. In the gels shown in Figure 16, especially in the polydisperse PEGylation gel, it is clearly seen that there was some amount of unPEGylated T4L that decreased as the molar excess of PEG was increased. This is less true with the discrete PEGylation, which appears to PEGylate more effectively, thereby leaving less T4L unPEGylated, which would result in less activity overall, for every sample. These trends, predicted by the explanation that PEGylating a certain lysine or lysines kill activity by itself, are what is indeed seen in Figure 16. The activity seems to be related to the amount of unPEGylated material.

In order to further investigate the above conundrum, a CD scan was acquired of selected PEGylated samples of T4L (same as above), along with an unPEGylated sample

and with simple solutions of PEGs, unattached to anything. Shown in Figure 17, the unPEGylated T4L sample produced a fine spectrum, but the other samples all exceeded the dynode voltage due to PEG's strong absorbance and thus, beyond that point, the spectra were inaccurate and not presented. No information was gleaned from this experiment and other characterizations were pursued because this was the point where it was discovered that the EnzChek® Assay might not accurately report on all types of Lysozyme activity.

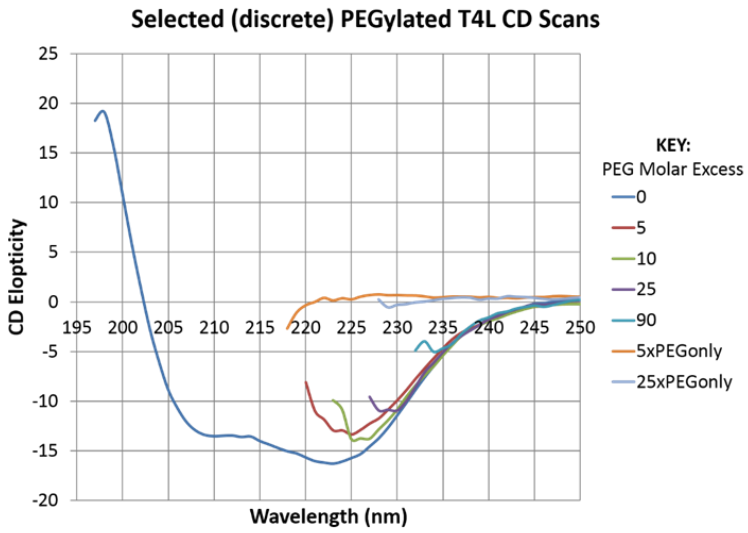

Figure 17. CD scans of PEGylated T4L of raw PEGs

The Imoto assay, described in the Methods section, is another lysozyme activity assay which works by measuring the disappearance of absorbance at 420 nm (yellow color) of a colorimetric reagent, $[Fe(CN)6]^{3-}$, that reacts with the digested substrate, glycol chitosan, eliminating its absorbance/color. The assay was shown to work when, as

a control, HEW lysozyme was used according to the protocol at different concentrations. These results in Figure 18 show a decrease in absorbance at 420 nm with increasing concentration of HEW lysozyme.

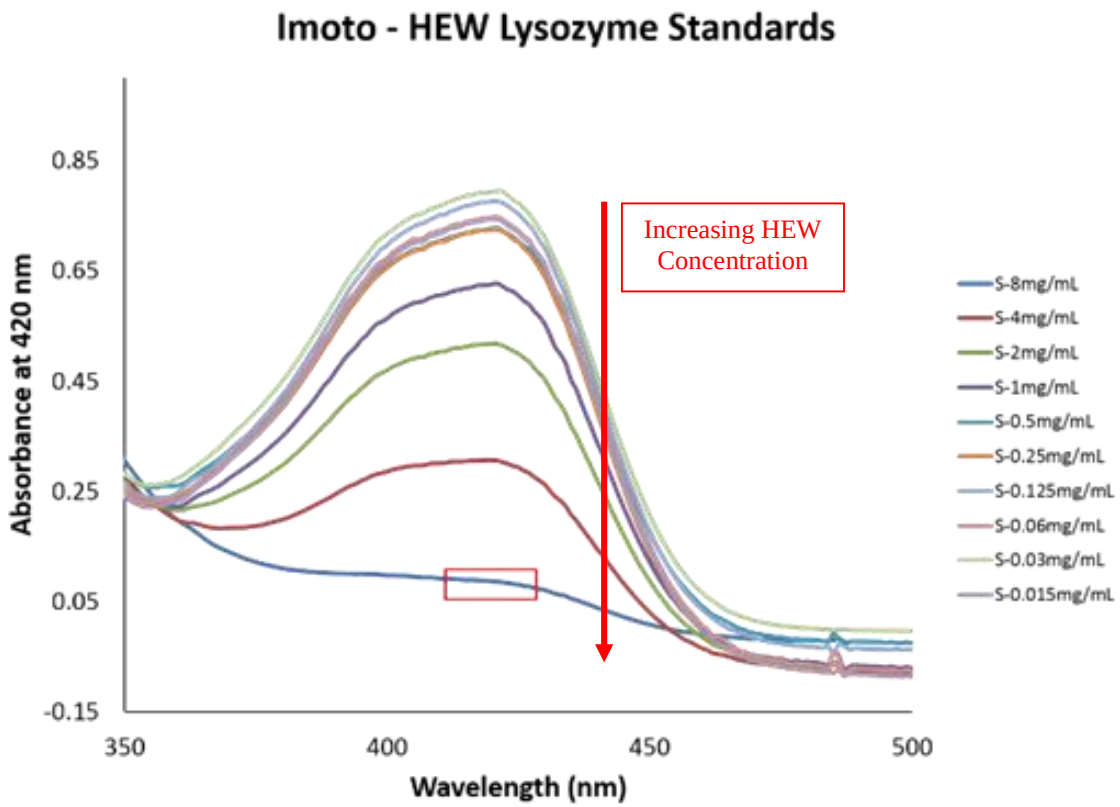

Figure 18. Imoto assay performed on hen egg white lysozyme standards

The experiment was then performed on T4L, with unPEGylated and PEGylated samples. Figure 19 shows that, basically, all of the signals are in the background noise, i.e. none of the samples showed any appreciable activity. This could be because the concentrations of the samples of T4L were too low and thus not enough substrate was

turned over to show any decrease in absorbance at 420 nm, or because the substrate, glycol chitosan, is not digestible by T4L.

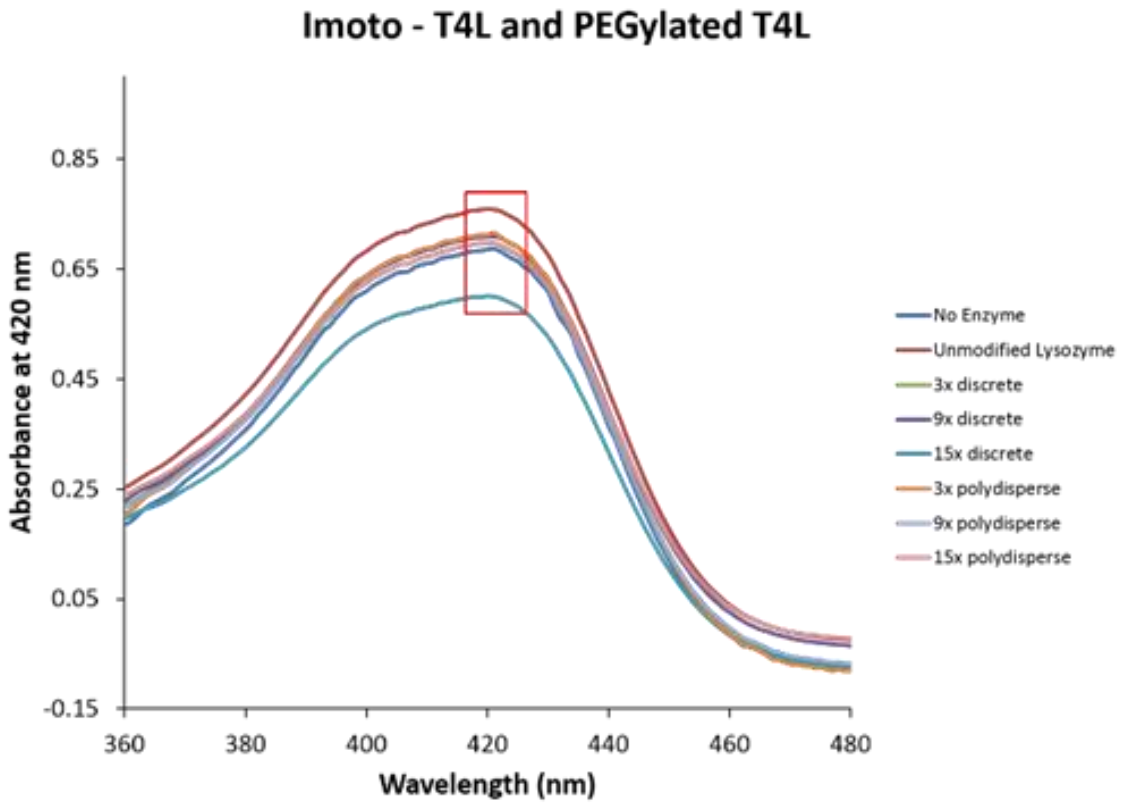

Figure 19. Imoto assay performed on T4L, PEGylated and not

In an attempt to decipher the meaning of this results of the Imoto assay, it was slightly modified so that it was performed under conditions similar to the EnzChek® Assay (40 °C was changed to 37 °C and the reaction buffer was changed to that of the EnzChek® Assay) while the EnzChek® Assay itself was repeated in parallel. Figure 20 shows that while T4L does not produce as much fluorescence as HEW lysozyme, it still

shows enough fluorescence over the background that its activity is not in question via the EnzChek® Assay.

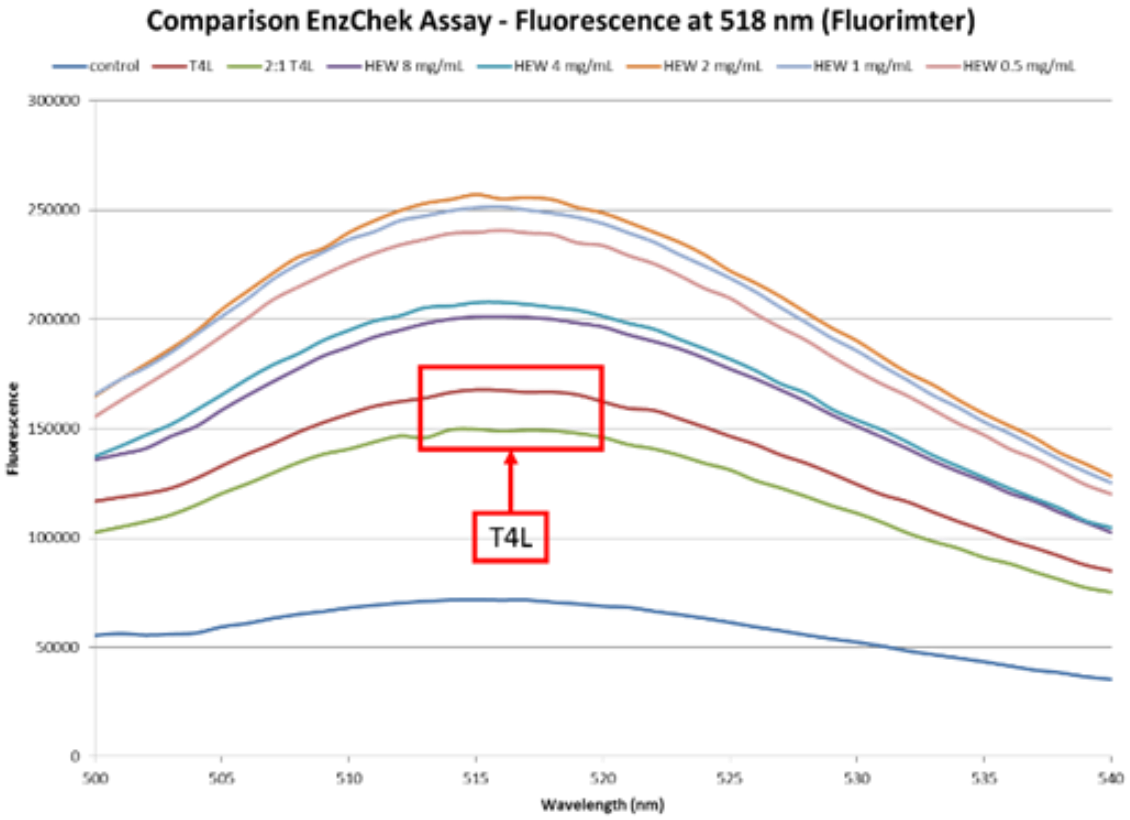

Figure 20. Repeat of EnzChek® assay; shows T4L activity

However, in the modified Imoto procedure, the results of which are shown in Figure 21, once again, the depletion of absorbance at 420 nm by any T4L sample, i.e. the activity, is not appreciable/is in the background, while the same HEW lysozyme samples show remarkable depletion of absorbance at 420 nm. This experiment did nothing to decipher the results of the pure Imoto procedure, but it proved that it works for active hen egg white lysozyme samples.

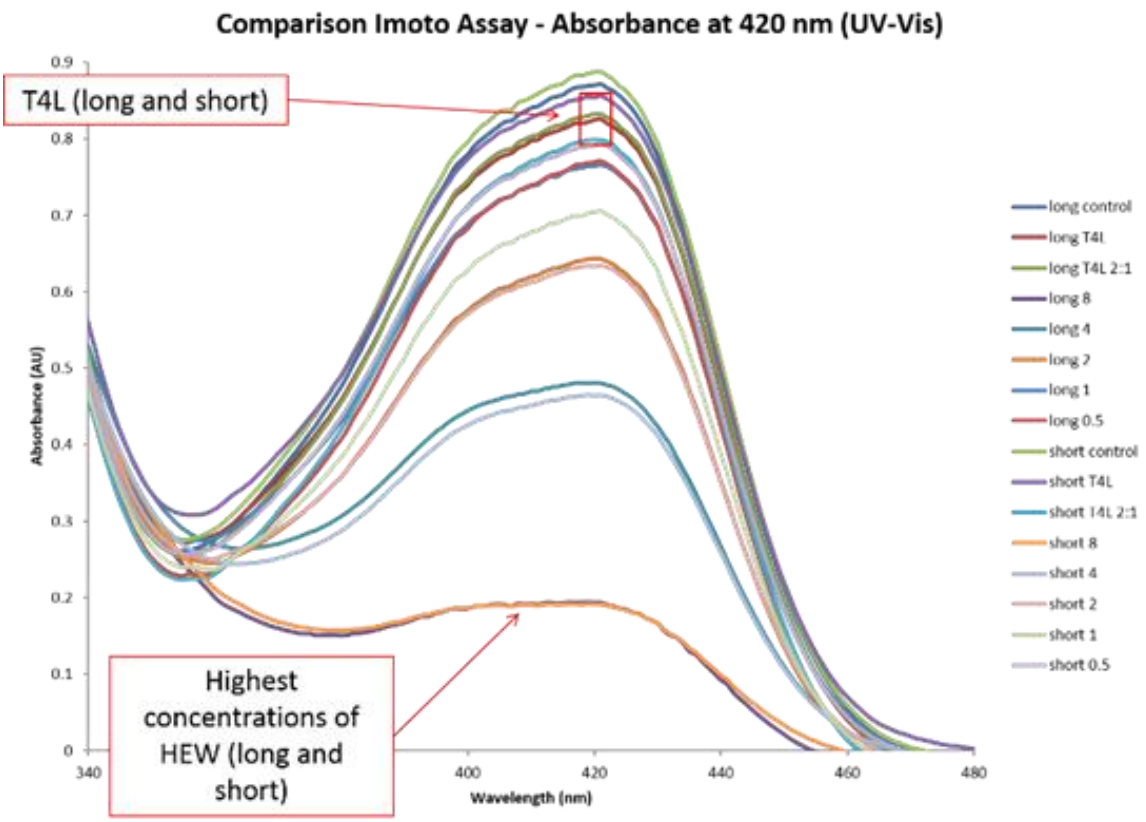

Figure 21. Repeat of Imoto assay under EnzChek conditions

The nature of T4L's limited response in the Imoto assay, whether due to inactivity against glycol chitosan or due to a low concentration, was not investigated further because at the time of this final experiment, it was discovered that 3E8.scFv and 3E8cys.scFv could be produced at a high enough level using pHLIC and C43(DE3), meaning that T4L had no further use as a model protein for PEGylation studies.

3E8.scFv was first nonspecifically PEGylated at lysines with the same 1.8 kD discrete PEG as before. The lysines of 3E8.scFv are depicted in Figure 22 in orange with

the CDR, or binding site, shown in purple. Only the 12 lysines not in the linker are shown. More lysines exist in the peptide linker, but are not shown.

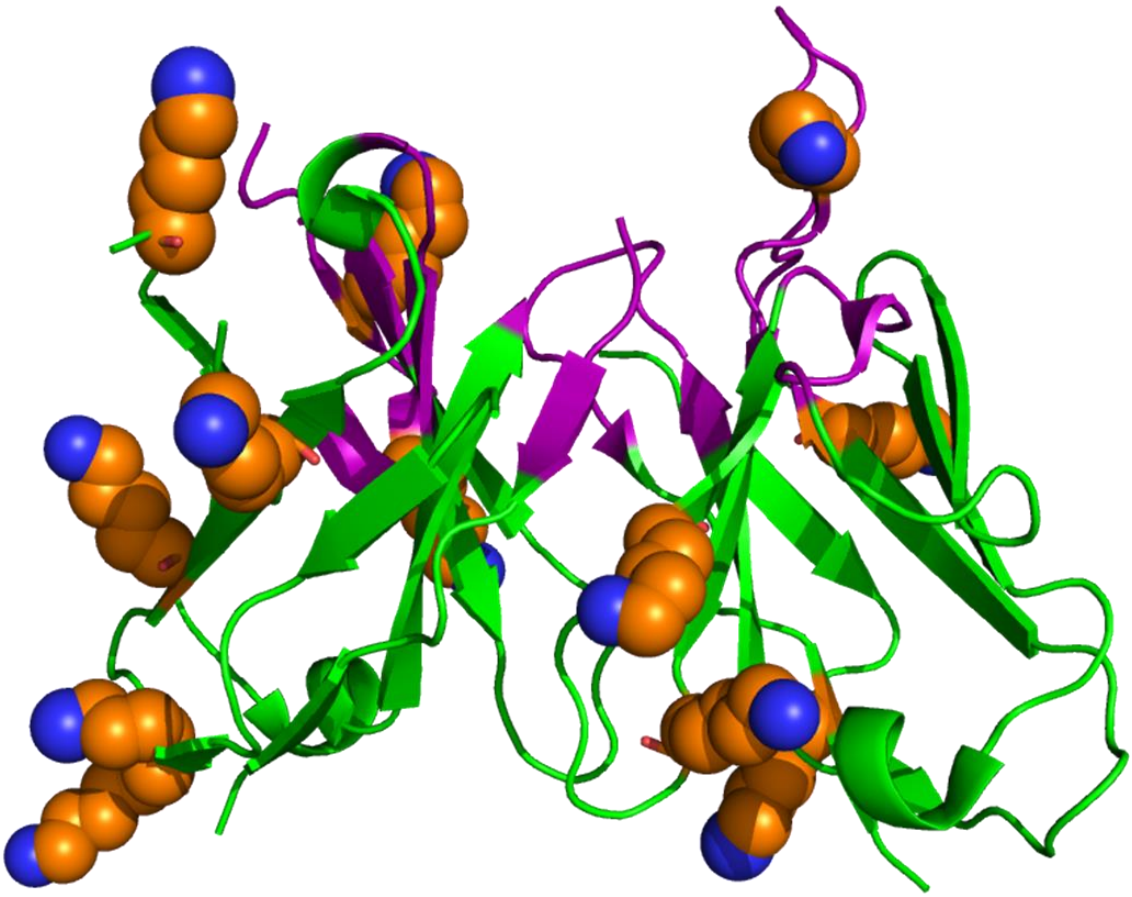

Figure 22. 3E8.scFv with orange/blue Lys and purple CDR

Figure 23 shows that, for the purposes of a study of various types and sizes of PEGs, 2x molar excess produced what was designated to be the “low” average number of attached PEGs while 16x molar excess produced what was designated to be the “high” average number of attached PEGs.

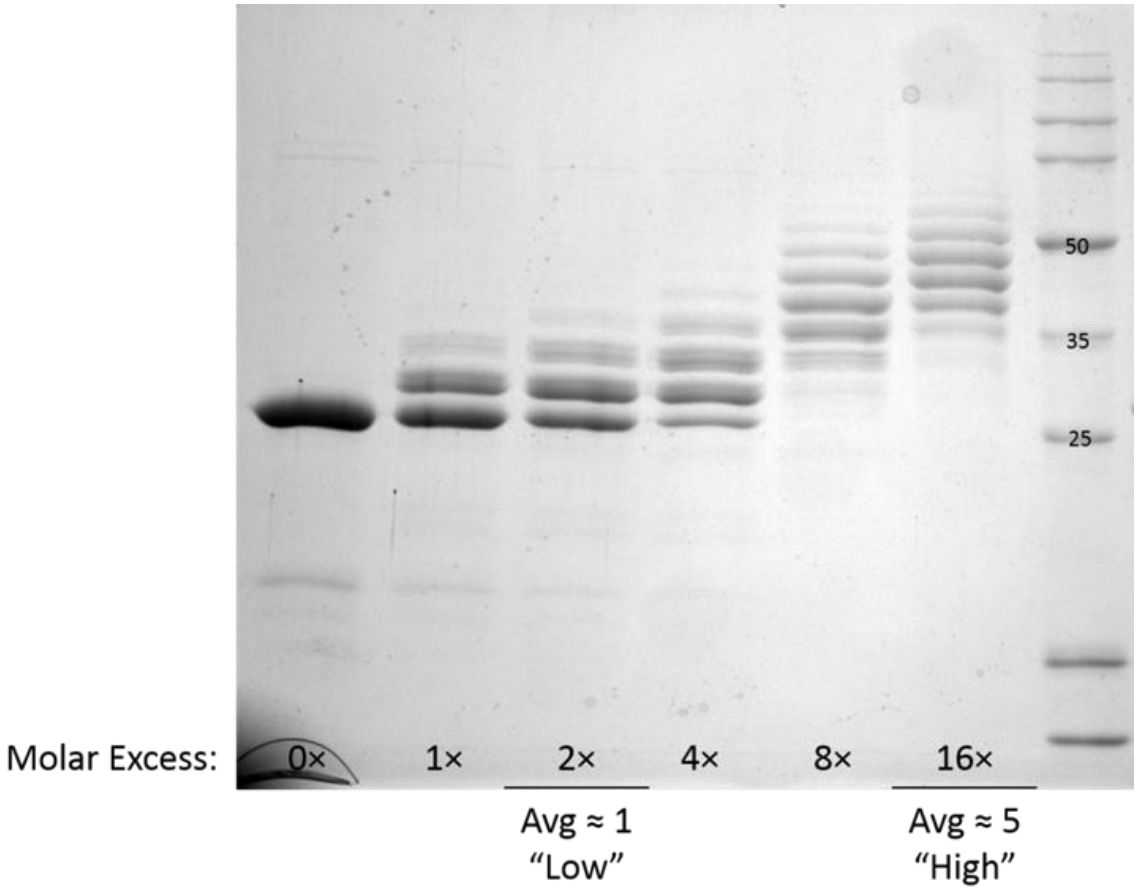

Figure 23. Nonspecific PEGylation of 3E8.scFv with 1.8 kD discrete NHS-ester PEG

A set of six different PEGs was chosen and is shown in Figure 24. Each PEG was given a letter as a label. PEGs B, D, E, F, and X were discrete PEGs with the shown molecular weights (Quanta BioDesign), while PEG Y was the same 2 kD polydisperse PEG (Creative PEGWorks) as before. (PEG X was the same discrete PEG used before as well.)

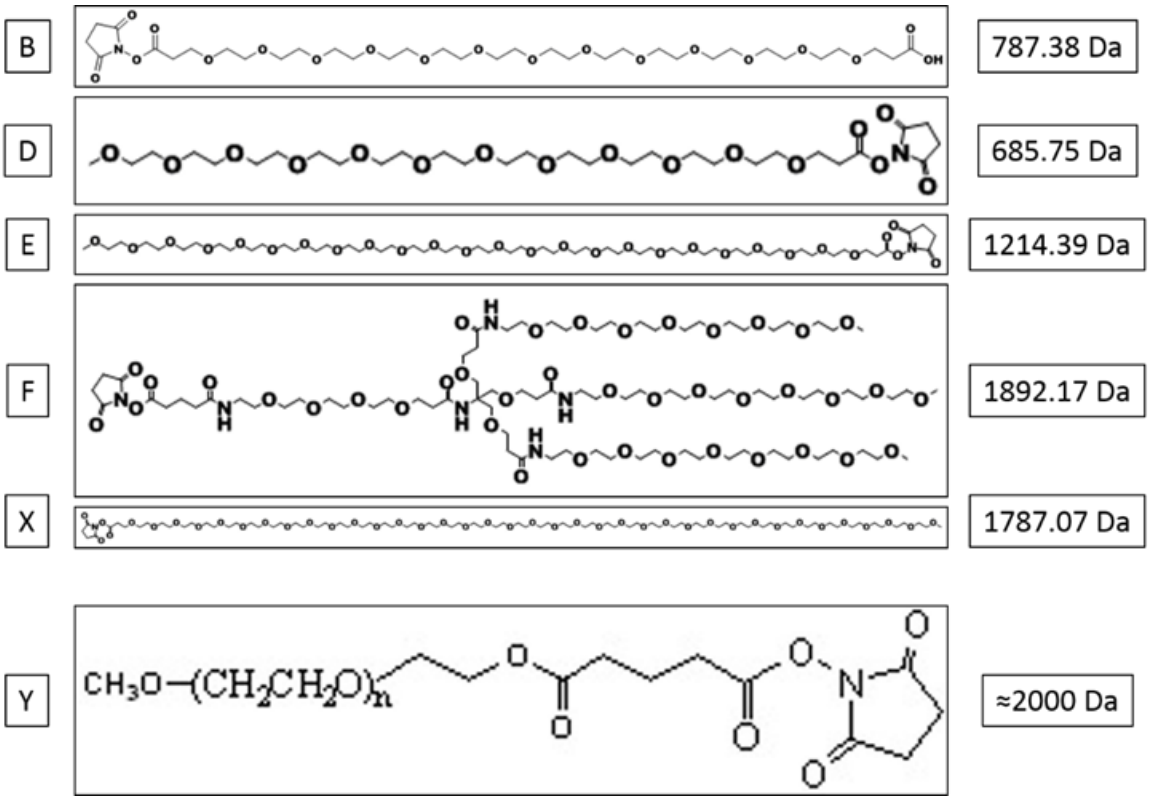

Figure 24. Six NHS-ester PEGs of various size, shape, and charge

Each PEG above was reacted with 3E8.scFv at 2x and 16x molar excess (low load, or "L," and high load, or "H," respectively), keeping the total volume and final concentration of 3E8.scFv the same in every reaction. The results of these PEGylations, after dialysis, are shown in Figure 25. (The sample that was PEGylated with PEG Y at high load was lost in the dialysis step due to a hole in the dialysis cassette.)

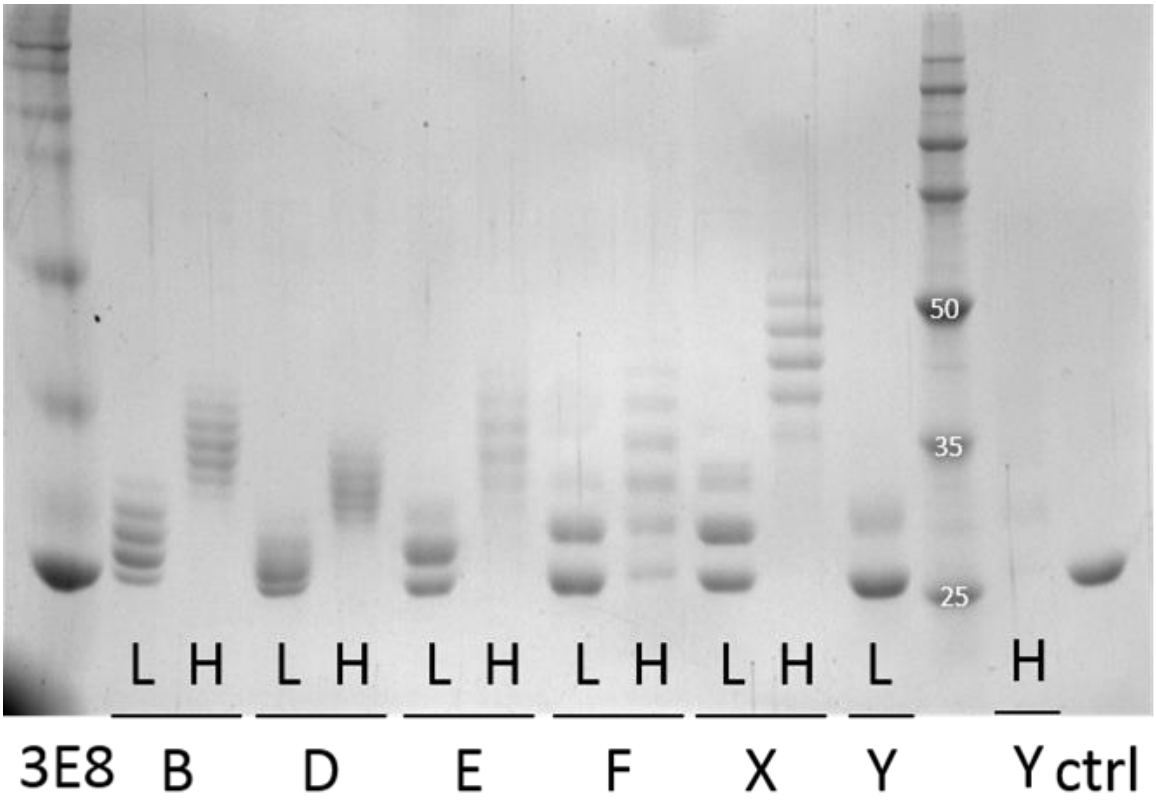

Figure 25. Nonspecific PEGylation of 3E8.scFv with the six PEGs from Figure 16

The samples shown in Figure 25 were then characterized using DSF. Differential scanning fluorimetry, or DSF, uses SYPRO® Orange dye, which, when exposed to a hydrophobic environment, fluoresces. In DSF, protein samples are heated up, causing them to unfold. The cores of proteins very often contain many hydrophobic residues, and so, as proteins are heated up and unfolded, more and more hydrophobic residues are exposed to solution. Therefore, as the samples are heated up, SYPRO® Orange binds to more and more hydrophobic residues and increasingly fluoresces, resulting in a higher signal. Figures 26 and 27 show the DSF melting curves of the PEGylated 3E8.scFv samples at low loads and at high loads, respectively. All of the samples PEGylated at low

loads appear to melt at the same temperature as unPEGylated 3E8.scFv, shown in the thick black line, and thus the stability of 3E8.scFv is not decreased with low levels of PEGylation. At high PEGylation loads, however, all of the samples have lower melting temperatures than unPEGylated 3E8.scFv, indicating that higher loads of PEGylation actually decrease the stability of 3E8.scFv by a small amount.

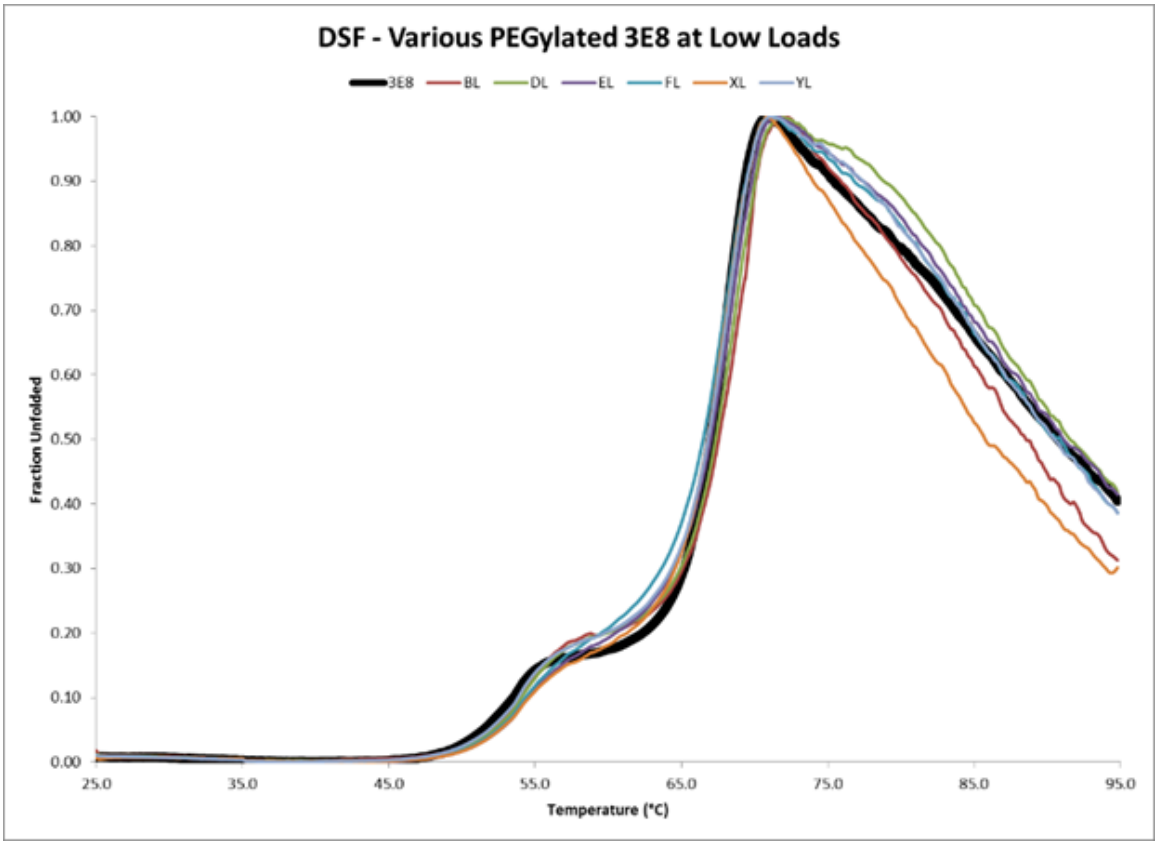

Figure 26. DSF spectrum of 3E8.scFv PEGylated at low load

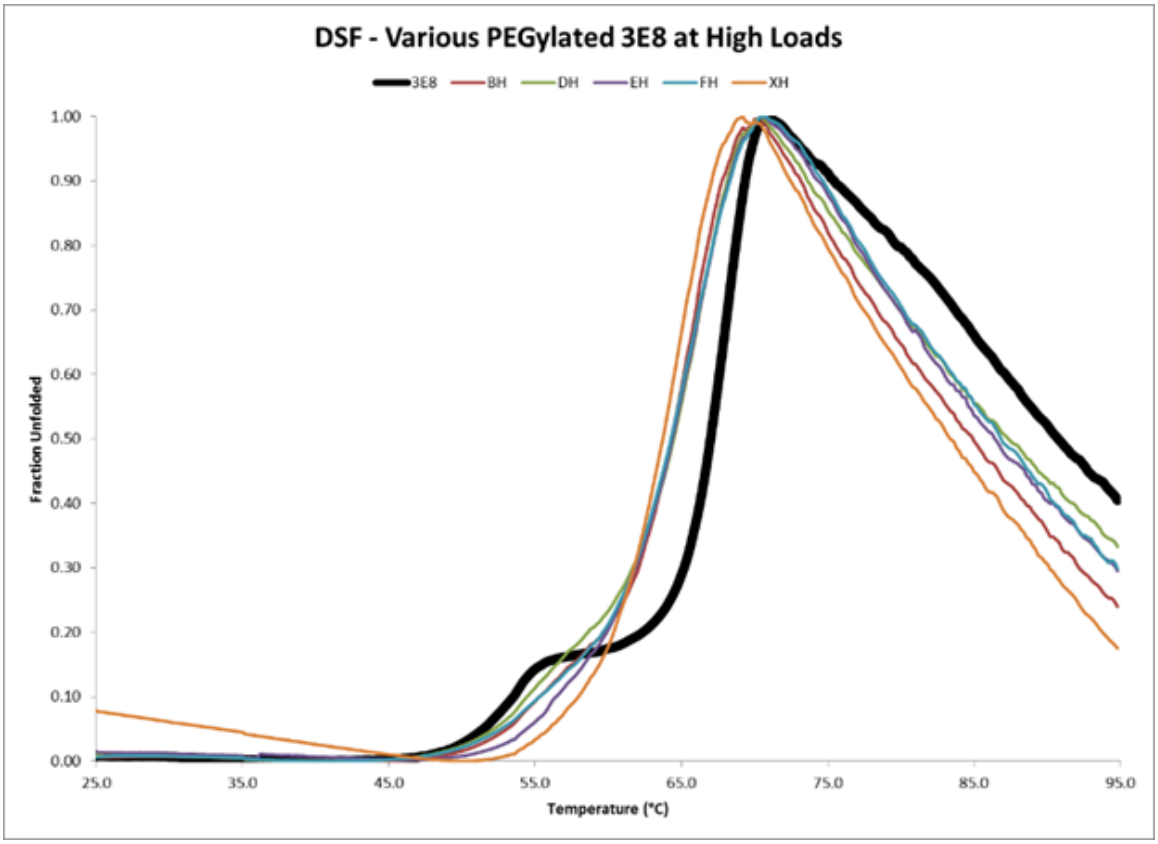

Figure 27. DSF spectrum of 3E8.scFv PEGylated at high load

Surface plasmon resonance, or SPR, was then used to characterize the effects of PEGylation on the binding of 3E8.scFv to the proper substrate, Sialyl-Tn. Example SPR spectrograms are shown in Figures 28 and 29, which show the binding behavior of the low and high load PEGylated samples (respectively) using PEG X, the 1.8 kD discrete PEG. The corresponding lane from the gel in Figure 23 is shown in the upper right corner of each Figure. The different traces, color-coded, represent different concentrations of sample that were run. These were suggested by the programmed protocol.

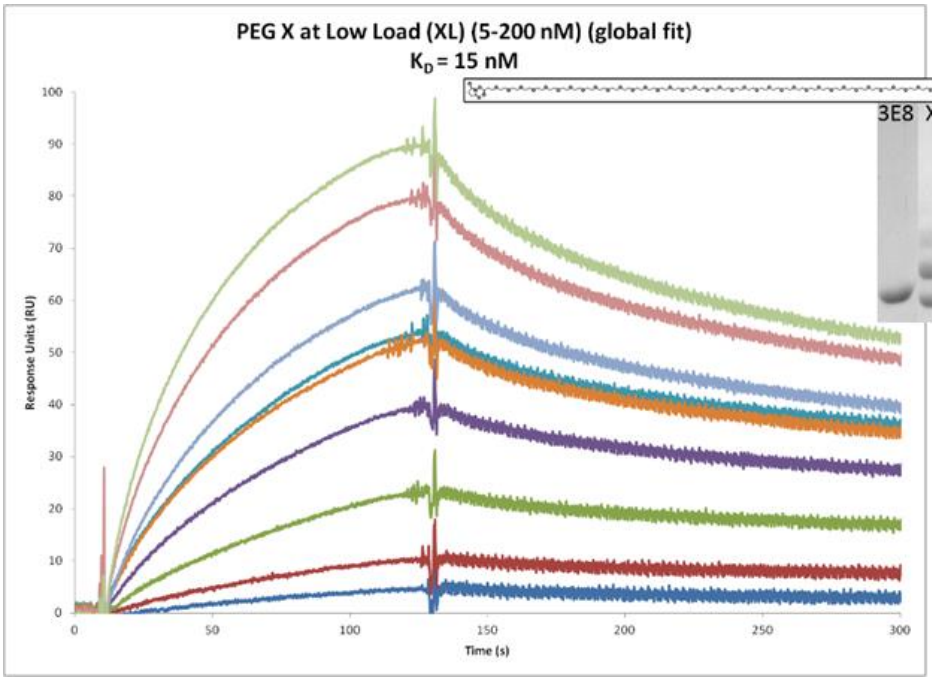

Figure 28. SPR of 3E8.scFv PEGylated with PEG X at low load

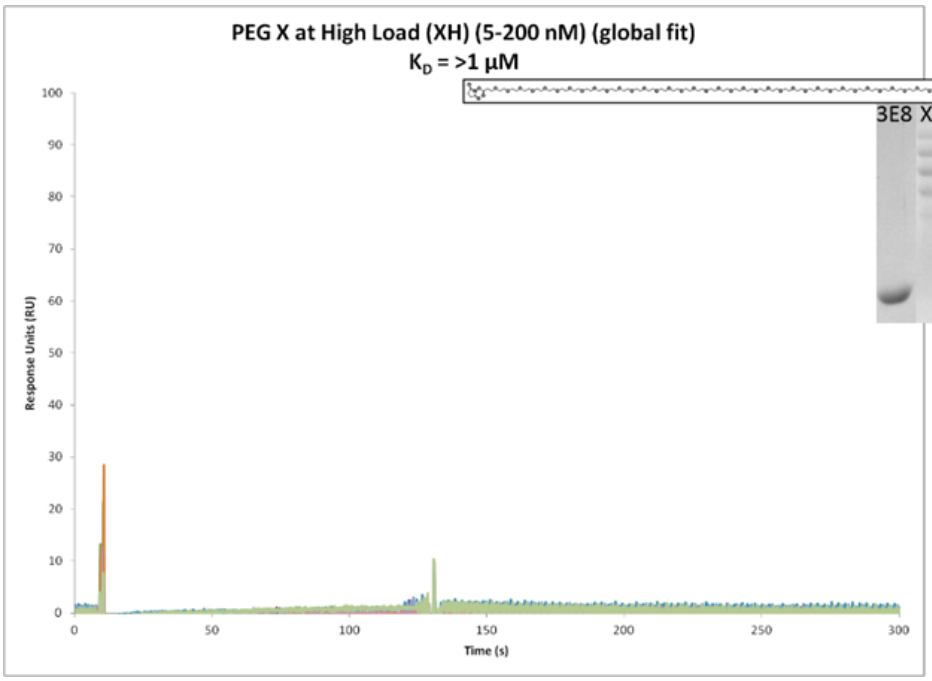

Figure 29. SPR of 3E8.scFv PEGylated with PEG X at high load

The results of the SPR experiment for all of the PEGylated samples are shown in Table 1. Similarly to the trend in stability with PEGylation loads, the trend in binding activity seems to be that at higher loads of PEG, 3E8.scFv loses much, if not all, of its binding affinity.

Sample	K_D	
3E8.scFv	12 nM	
PEG	**Low**	**High**
B	13 nM	>1 µM
D	31 nM	>1 µM
E	30 nM	230 nM
F	26 nM	41 nM
X	15 nM	>1 µM
Y	20 nM	-

Table 1. K_D values of 3E8.scFv PEGylated at low and high load with various PEGs

The same confounding question about whether high loads of PEGylation in general ablates activity/binding or whether specific lysines that have a great effect on activity/binding are more likely to be PEGylated at high loads that was present in the T4L PEGylation experiments is present again in these DSF and SPR PEGylation experiments. As previously stated, this issue is being pursued further, but in an attempt to get some definitive information about what PEGylation does to binding and stability, specific PEGylation using maleimide chemistry and cysteine residues was pursued using 3E8cys.scFv.

4.3 Specific PEGylation at Cysteines and Characterization

Once it was known that using the pHLIC plasmid in the C43(DE3) strain could produce a moderate amount of 3E8cys.scFv, it started being produced in mass quantities so that PEGylation could be studied in isolation, via single PEGylation at the added free cysteine, which is depicted in Figure 30, in red.

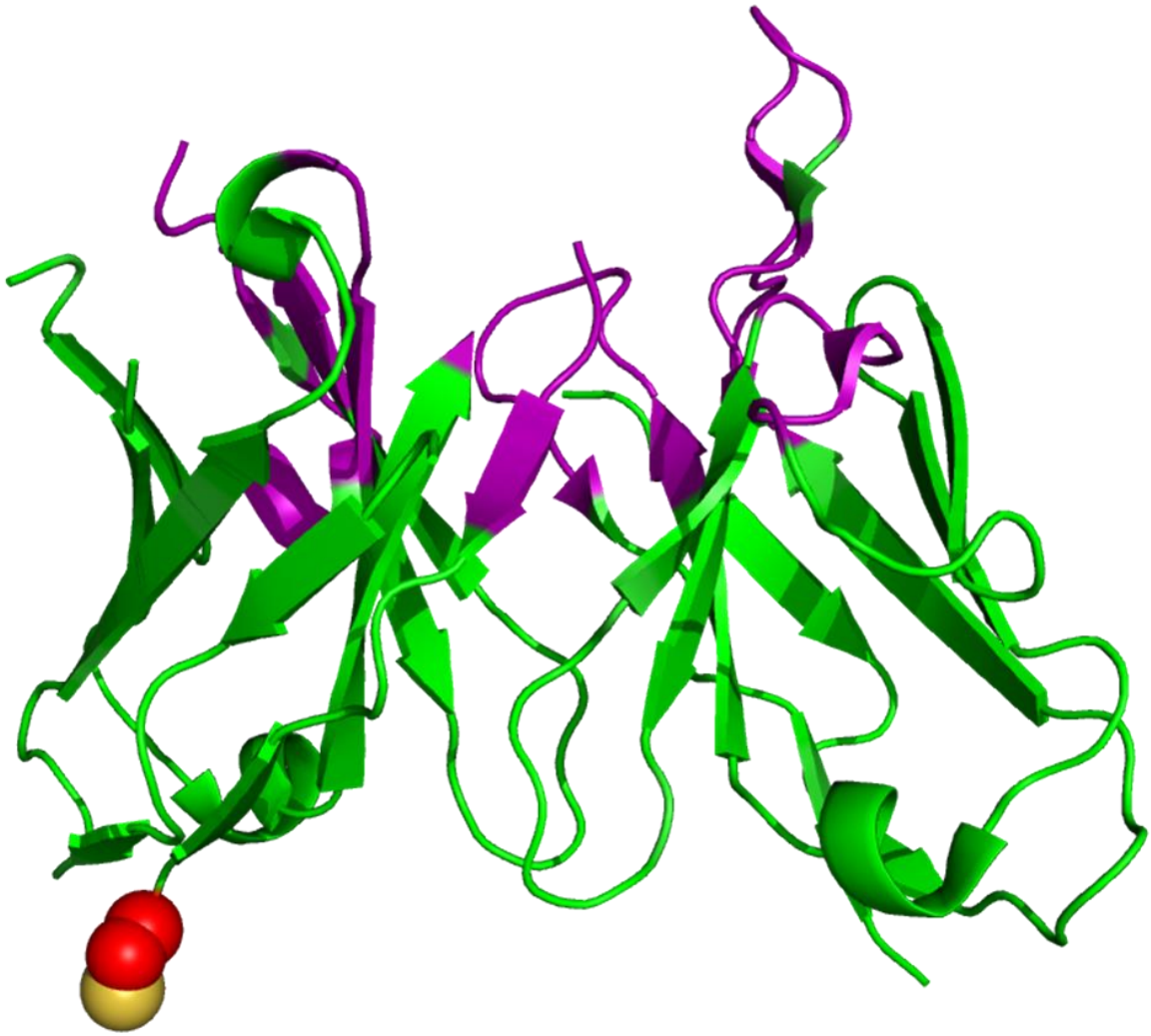

Figure 30. 3E8cys.scFv with red/yellow C-terminal free Cys and purple CDR

In order to get the sizes of PEG desired, polydisperse PEGs had to be used because Quanta BioDesign does not routinely synthesize PEGs larger than about 10 kD. The series of PEGs that was used was designed to study the differences in size and in shape, so maleimide PEGs of 5 kD, 20 kD, and 40 kD were used (JenKem Technology USA). All of these were linear PEGs (the normal configuration), but in addition, a 40 kD Y-shaped branched PEG was also used (JenKem Technology USA), a picture of which is shown Figure 31.

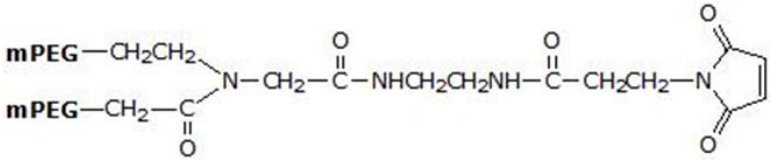

Figure 31. Basic Structure of Y-shaped PEG from JenKem

Four samples of 3E8cys.scFv were PEGylated at 50x molar excess overnight at room temperature with each of the four PEGs mentioned above. Additionally a control sample, labeled “ctrl,” was treated the same way as the PEGylated samples but no PEG was added, only buffer. The initial gel is shown in Figure 31. Large PEGs do not run well on SDS-PAGE gels because SDS does not bind well to them, so it is difficult to see the extent of PEGylation in Figure 31.

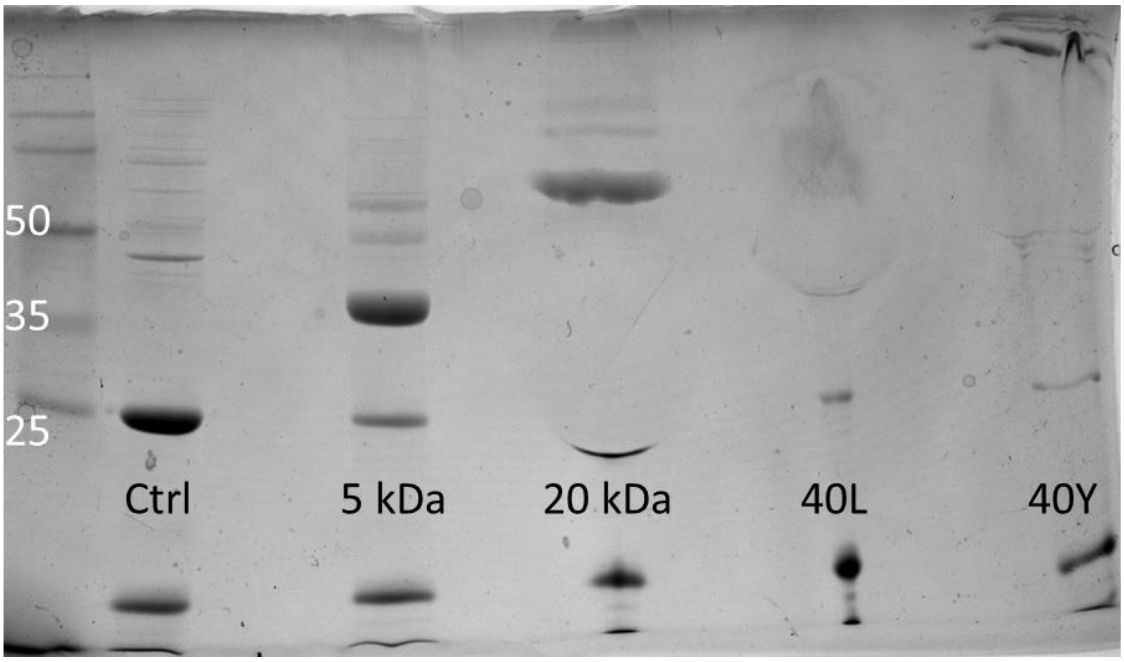

Figure 32. Specific PEGylation of 3E8cys.scFv with four maleimide PEGs

The PEGylation samples were buffer swapped into 50 mM potassium acetate buffer in order to perform ion exchange. The elution profiles of the five samples from ion exchange are shown in Figures 32-36, and the fractions combined as the purified product are indicated with the red boxes.

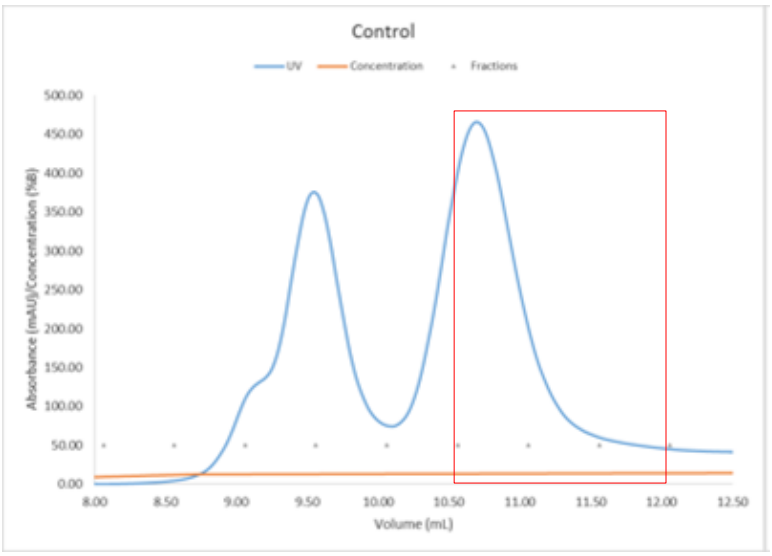

Figure 33. Ion exchange (IEX) elution profile of unPEGylated 3E8cys.scFv

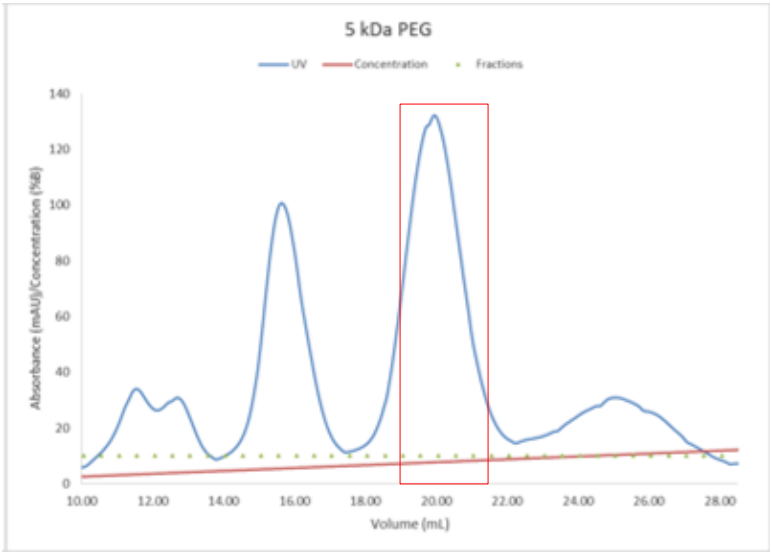

Figure 34. IEX elution profile of 3E8cys.scFv PEGylated with 5 kD PEG

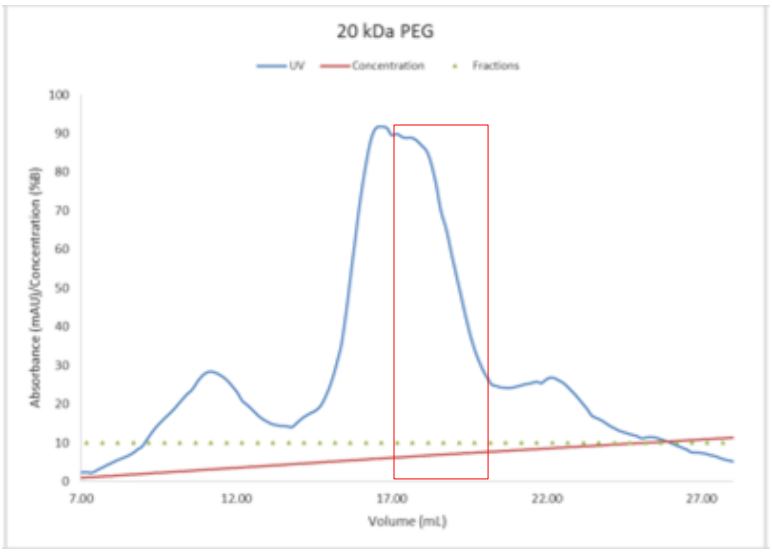

Figure 35. IEX elution profile of 3E8cys.scFv PEGylated with 20 kD PEG

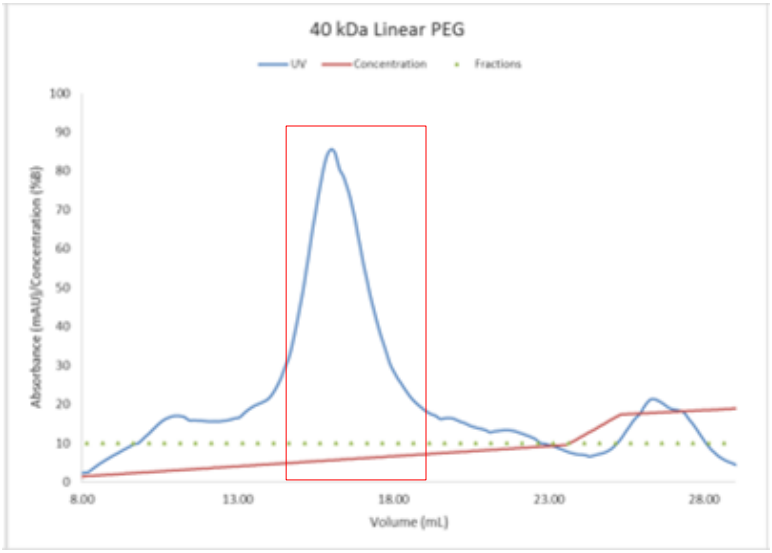

Figure 36. IEX elution profile of 3E8cys.scFv PEGylated with linear 40 kD PEG

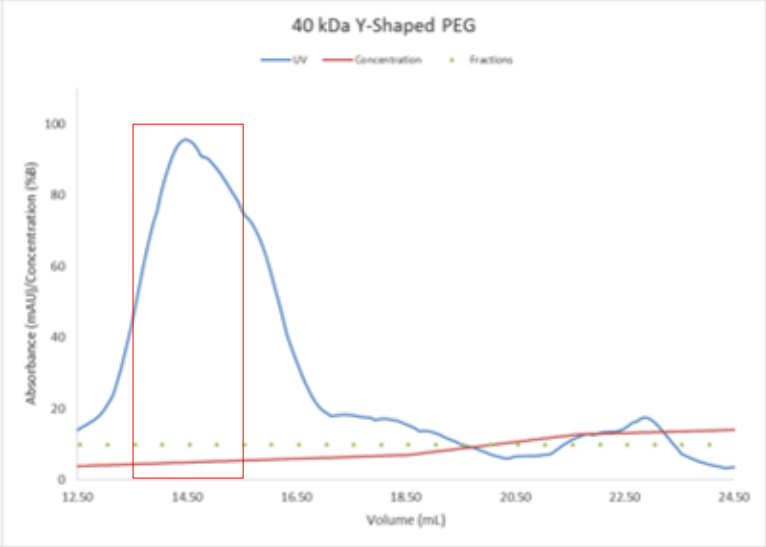

Figure 37. IEX elution profile of 3E8cys.scFv PEGylated with Y-shaped 40 kD PEG

After the fractions were recombined, they were concentrated down to around 1 mL using the same concentrators as mentioned in methods and buffer swapped into PBS using NAP 10 columns. The purified and concentrated samples were then run on a gel to determine concentration by comparison to the known concentrations of protein in the ladder: the 50 kD band is 1 µg and the 35 and 25 kD bands are each ½ µg. The gel is shown in Figure 37.

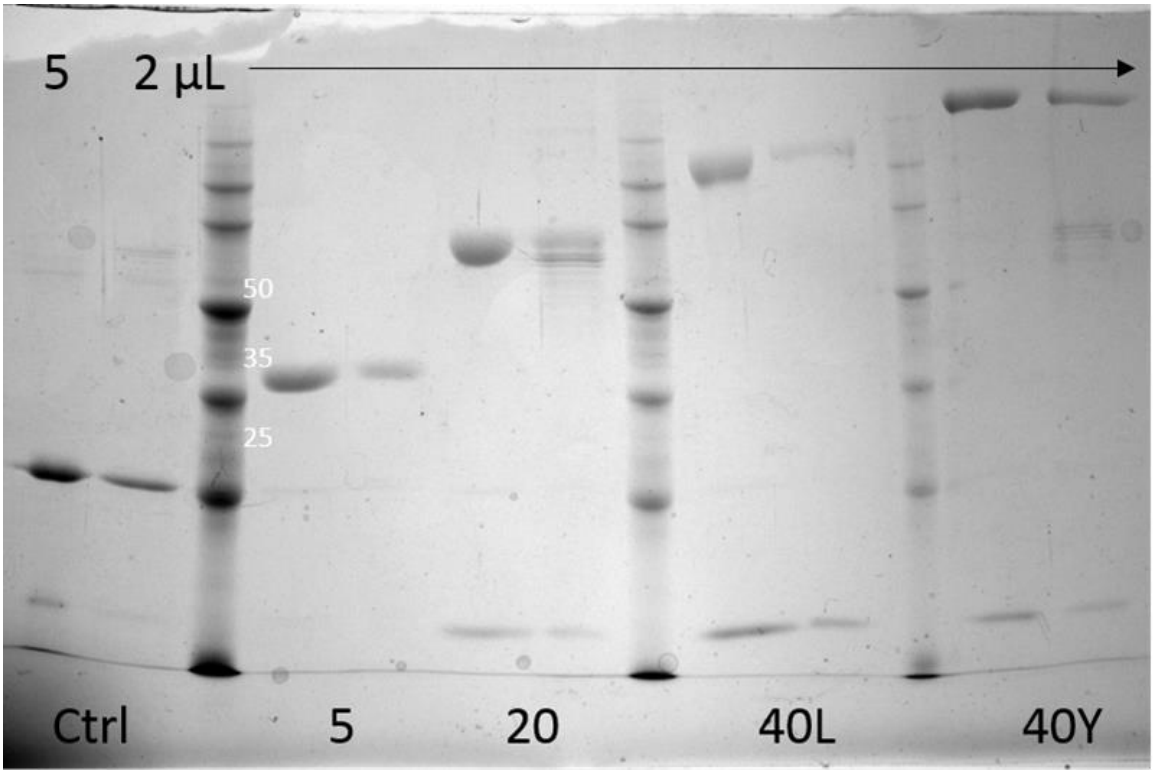

Figure 38. Gel of IEX purified PEGylated 3E8cys.scFv samples

Gel filtration was then performed on the five samples, injecting 200 µL of each. The results, shown in Figure 38, indicate that each of the five samples appear to be monomers. The apparent molecular weights are inaccurate, however, likely due to the fact that the standard curve was calculated using the elution profiles of globular, spherical proteins, whereas 3E8cys.scFv is more complicated than that, in addition to the fact the PEGs are less dense than protein, meaning PEG-protein conjugated will have a larger volume than an equivalent molecular weight of pure protein.

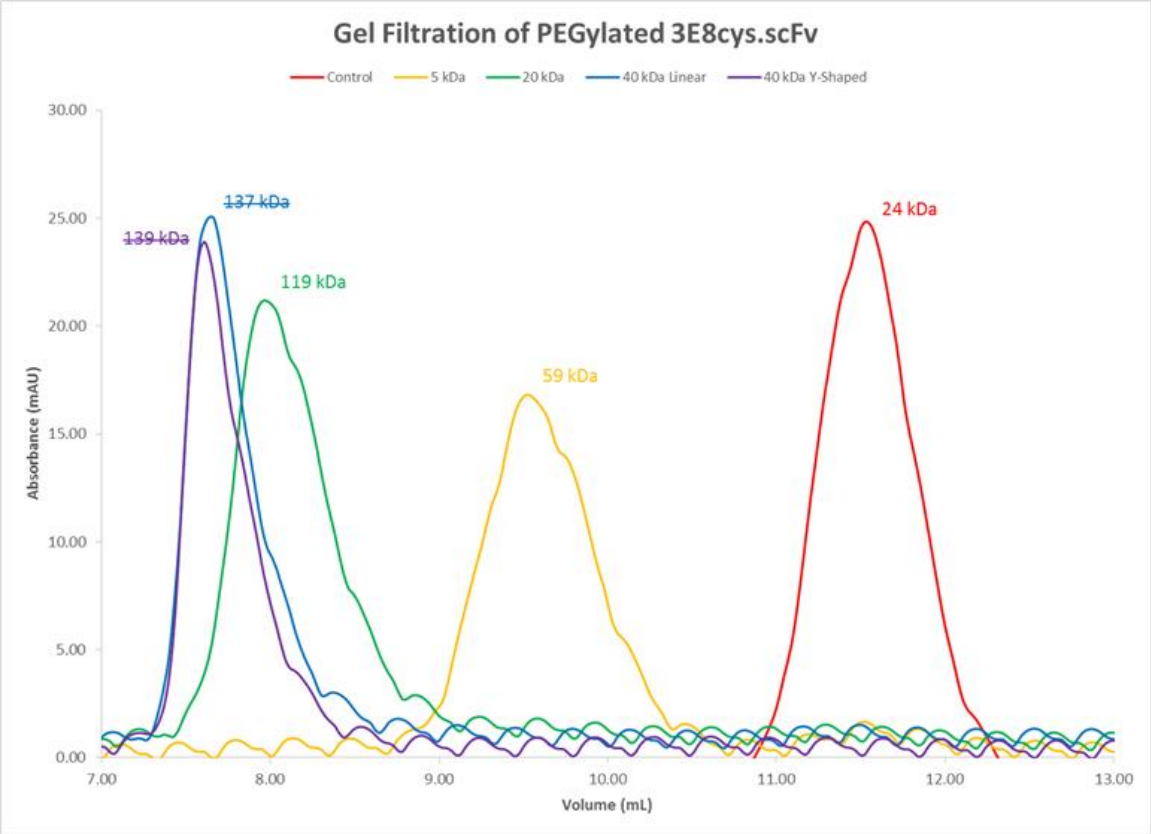

Figure 39. Gel filtration elution profiles of PEGylated 3E8cys.scFv

The DSF profile of the five samples, shown in Figure 39, was rather unexpected and difficult to decipher. The presence of the first transition, which is seemingly visible in the unPEGylated samples but accentuated in the PEGylated samples (with the exception of the samples PEGylated with the 5 kD PEG), is somewhat of a mystery. It could represent the dissociation of the two domains of the antibody fragment while the second transition, which is what we consider to be the main transition for the unPEGylated 3E8cys.scFv and 3E8.scFv, could represent the unfolding of the individual

domains in the proteins. Additionally, the first transition could represent some interaction between the PEGs and the dye. It's origin is currently unknown.

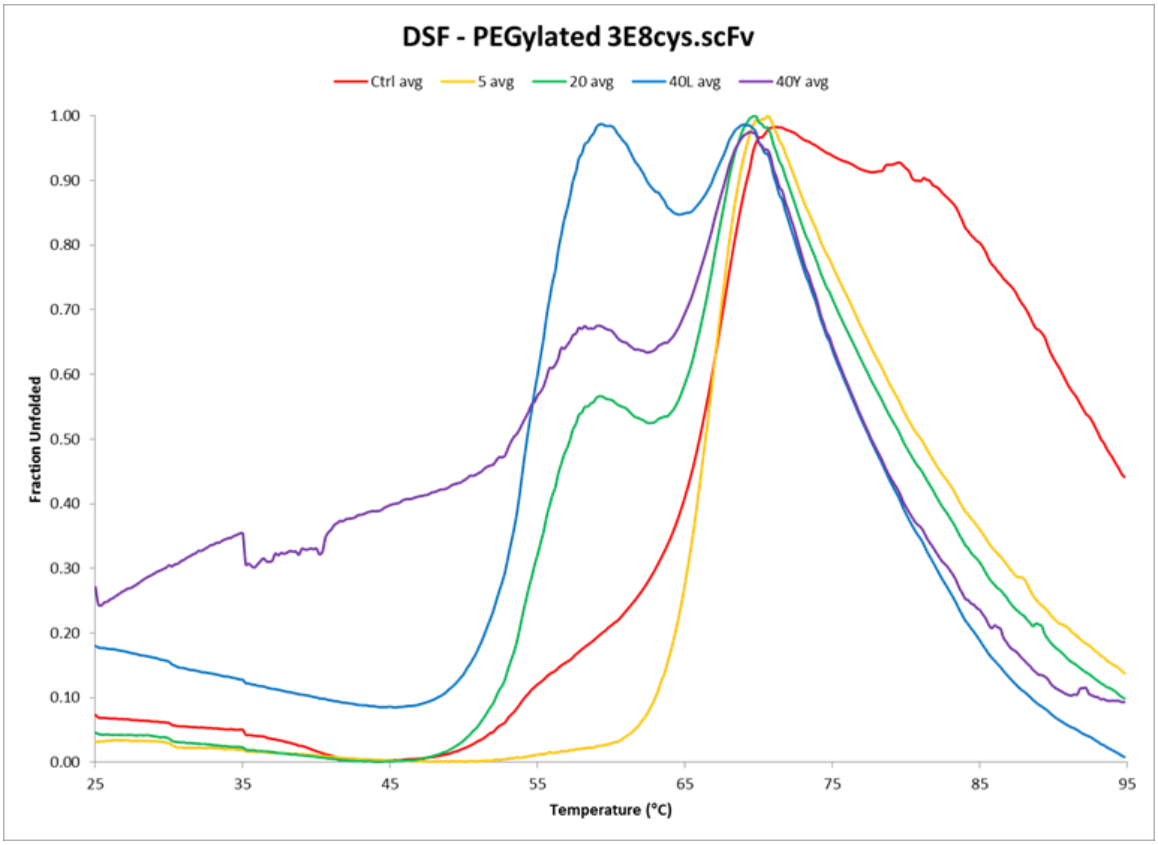

Figure 40. DSF melting profiles of PEGylated 3E8cys.scFv

SPR was also performed on samples prepared before those analyzed above, the results of which are shown in Table 2. UnPEGylated 3E8cys.scFv was shown to have a K_D of around 40 nM and 3E8cys.scFv samples PEGylated with the same 40 kD linear and Y-shaped PEGs as above were shown to not have decreased binding.

Sample	K_D
3E8cys.scFv	39 nM
40L kDa	41 nM
40Y kDa	44 nM

Table 2. K_D values of 3E8cys.scFv and two PEG conjugates

Conclusions and Future Directions

T4L was used as a preliminary model for 3E8.scFv. It was produced at high yield and was then nonspecifically PEGylated. The resulting PEG conjugates were tested for activity using the EnzChek® Lysozyme Assay Kit. The assay worked but the results were not conclusive. It appeared that the activity of each of the PEGylated samples corresponded to the amount of unPEGylated T4L in each sample. This observation lead to the thought that any amount of PEGylation was detrimental to binding. In an attempt to remedy this, a different lysozyme activity assay, discussed as the Imoto assay, was attempted. This assay worked on the standard HEW lysozyme samples but not on any T4L samples, leading to the conclusion that the substrate being used was not a viable substrate for T4L. At this point, the expression and purification of 3E8.scFv and 3E8cys.scFv was optimized and T4L as s model protein was no longer needed.

3E8.scFv, previously extensively characterized and now being produced in reasonable high yields, was then PEGylated nonspecifically as T4L had been. The resulting PEG conjugates were studied for binding activity via SPR and for stability via DSF. SPR revealed that low loads of PEGylation (an average of around one or two PEGs per molecule) did not affect binding much, if at all, while higher loads of PEGylation (an average of about five attached PEGs per molecule) resulted in an almost complete ablation of binding. DSF revealed that low loads of PEGylation did not affect stability

much, if at all, while higher loads seemed to decrease the melting temperature by a few degrees. These results were somewhat difficult to interpret because exactly which lysines were PEGylated was not knowable based simply on SDS-PAGE analysis. It could be, for example, that the PEGylation of a specific lysine in the binding site was responsible for the complete ablation of binding while PEGylating every other lysine would have no effect on binding. In order to eliminate some of these variables and to study PEGylation in a more pure form, a version of 3E8.scFv with an extra free cysteine engineered onto the C-terminus, called 3E8cys.scFv, was to be used.

3E8cys.scFv was also being produced in high yields at this point, so it was an easy transition to PEGylating this version of 3E8.scFv. It was PEGylated specifically at the free cysteine using maleimide PEGs. This meant that only a single PEG, of known size, was attached to each 3E8cys.scFv molecule after the PEGylation reaction. This removed the question of which residues might have been preferentially PEGylated and allowed a more comprehensive study on PEGylation as a modification. Previous SPR results indicated no decrease in binding when a single 40 kD PEG (linear or Y-shaped) was attached. Gel filtration showed that four samples of 3E8cys.scFv each singly PEGylated with one of a 5 kD, a 20 kD, a linear 40 kD, and Y-shaped 40 kD PEG were all still monomers with no aggregation. DSF scans of these PEGylated samples showed an interesting unfolding profile with a large transition that grew in before the original unfolding transition in the spectrum of 3E8cys.scFv. The nature of this is unknown but it could represent the dissociation of the two domains of 3E8cys.scFv before the unfolding

of the individual domains. Whatever it is, it appears that single PEGylation at the C-terminus with large PEGs (greater than 20 kD) changes how 3E8cys.scFv unfolds.

Future work entails finishing the biophysical characterization of the singly PEGylated 3E8cys.scFv samples with AUC, DSLS, and potentially SAXS. AUC measures sedimentation and will help to describe the shape of 3E8cys.scFv and its PEG conjugates by providing a hydrodynamic radius. DSLS is another stability study which relies upon aggregation of the protein of interest, measuring the amount of light that is transmitted through a protein sample being heated. However, because PEGs are thought to prevent or delay aggregation, this assay might simply reveal the aggregation characteristics of 3E8cys.scFv-PEG conjugates. SAXS is a structural technique which will reveal information about the size and shape of proteins by measuring how x-rays scatter at very small angles after being directed at the protein of interest. Specifically, this technique will be used to determine whether PEGs wrap around 3E8cys.scFv, which would result in a roughly spherical shape with little change in shape from the unPEGylated protein, or whether PEGs form a polymer-like bead near their attachment point, which would result in a "peanut" shape, more like two spheres next to each other.

Additionally, the nature of which of the lysines of 3E8.scFv are important in the realm of PEGylation will be investigated. To do this, several lysines which, if PEGylated, might cause a problem with the activity/binding of the protein (i.e. they are near the binding site), have been mutated individually to arginines. If any of these single mutants display binding activity, they will be PEGylated in a fashion similar to the nonspecific PEGylation studies presented in this thesis. If the resulting PEG conjugates still bind, the

mutated lysine could have been the problem. Additionally, a study to determine which lysines are being PEGylated (and hopefully, to determine in what order) will be conducted using some PEG-biotin derivative, a trypsin digest, and mass spectrometry. This will indicate which lysines are PEGylated in a nonspecifically PEGylated sample, and potentially, which lysines are preferentially PEGylated/PEGylated first (potentially due to activation).

References

1. Sun, D., Bloomston, M., Hinkle, G., Al-Saif, O. H., Hall, N. C., Povoski, S. P., Arnold, M. W. & Martin, E. W. (2007). Radioimmunoguided surgery (RIGS), PET/CT image-guided surgery, and fluorescence image-guided surgery: Past, present, and future. *J. Surg. Oncol.*, **96**, 297–308.

2. Bertsch, D.J., Burak, W.E. Jr., Young, D.C., Arnold, M.W. & Martin E.W. Jr. (1995). Radioimmunoguided Surgery system improves survival for patients with recurrent colorectal cancer. *Surgery*, **118**, 634-639.

3. Bertsch, D.J., Burak, W.E. Jr., Young, D.C., Arnold, M.W. & Martin E.W. Jr. (1996). Radioimmunoguided surgery for colorectal cancer. *Ann. Surg. Oncol.*, **3**, 310-316.

4. Gardner, B. (1987). Five-year survival after extended resection of colon cancer. *J. Surg. Oncol.*, **34**, 258-261.

5. Arnold, M.W., Young, D.C., Hitchcock, C.L., Schneebaum, S. & Martin E.W. Jr. (1995). Radioimmunoguided surgery in primary colorectal carcinoma: an intraoperative prognostic tool and adjuvant to traditional staging. *Am. J. Surg.*, **170**, 315-318.

6. Sickle-Santanello, B.J., O'Dwyer, P.J., Mojzisik, C., Tuttle, S.E., Hinkle, G.H., Rousseau, M., Schlom, J., Colcher, D., Thurston, M.O., Nieroda, C. *et al*. (1987). Radioimmunoguided surgery using the monoclonal antibody B72.3 in colorectal tumors. *Dis. Colon Rectum.*, **30**, 761-764.

7. Colcher, D., Milenic, D., Roselli, M., Raubitschek, A., Yarranton, G., King, D., Adair, J., Whittle, N., Bodmer, M. & Schlom, J. (1989). Characterization and biodistribution of recombinant and recombinant/chimeric constructs of monoclonal antibody B72.3. *Cancer Res*., **49**, 1738-1745.

8. Johnson, V.G., Schlom, J., Paterson, A.J., Bennett, J., Magnani, J.L. & Colcher, D. (1986). Analysis of a human tumor-associated glycoprotein (TAG-72) identified by monoclonal antibody B72.3. *Cancer Res.,* **46**, 850-857.

9. Thor, A., Ohuchi, N., Szpak, C.A., Johnston, W.W. & Schlom, J. (1986). Distribution of Oncofetal Antigen Tumor-associated Glycoprotein-72 Defined by Monoclonal Antibody B72.3. *Cancer Res.*, **46**, 3118-3124.

10. Colcher, D., Milenic, D.E., Ferroni, P., Carrasquillo, J.A., Reynolds, J.C., Roselli, M., Larson, S.M. & Schlom, J. (1990). In Vivo Fate of Monoclonal Antibody B72.3 in Patients with Colorectal Cancer. *J. Nucl. Med.*, **31**, 1133-1142**.**

11. Colcher, D., Hand, P.H., Wunderlich, D., Nuti, M., Teramoto, Y.A., Kufe, D. & Schlom, J. (1983). Monoclonal antibodies to human mammary carcinoma associated antigens and their potential uses for diagnosis, prognosis, and therapy. *Lab. Res. Methods Biol. Med.,* **8**, 215-258.

12. Colcher, D., Hand, P.H., Nuti, M. & Schlom, J. (1983). Differential binding to human mammary and nonmammary tumors of monoclonal antibodies reactive with carcinoembryonic antigen. *Cancer Invest.*, **1**, 127-138.

13. Colcher, D., Zalutsky, M., Kaplan, W., Kufe, D., Austin, F. & Schlom, J. (1983). Radiolocalization of human mammary tumors in athymic mice by a monoclonal antibody. *Cancer Res.*, **43**, 736-742.

14. Muraro, R., Kuroki, M., Wunderlich, D., Poole, D.J., Colcher, D., Thor, A., Greiner, J.W., Simpson, J.F., Molinolo, A., Noguchi, P. *et al*. (1988). Generation and characterization of B72.3 second generation monoclonal antibodies reactive with the tumor-associated glycoprotein 72 antigen. *Cancer Res.*, **48,** 4588-4596.

15. Morrison, S.L., Johnson, M.J., Herzenberg, L.A. & Oi, V.T. (1984). Chimeric human antibody molecules: mouse antigen-binding domains with human constant region domains. *Proc. Natl. Acad. Sci. U.S.A.*, **81,** 6851-6855.

16. Jones, P.T., Dear, P.H., Foote, J., Neuberger, M.S. & Winter, G. (1986). Replacing the complementarity-determining regions in a human antibody with those from a mouse. *Nature*, **321**, 522-525.

17. Yoon, S.O., Lee, T.S., Kim, S.J., Jang, M.H., Kang, Y.J., Park, J.H., Kim, K.S., Lee, H.S., Ryu, C.J., Gonzales, N.R., Kashmiri, S.V., Lim, S.M., Choi, C.W. & Hong, H.J. (2006). Construction, affinity maturation, and biological characterization of an anti-tumor-associated glycoprotein-72 humanized antibody. *J. Biol. Chem.*, **281**, 6985-6992.

18. Veronese, F.M. & Pasut, G. (2005). PEGylation, successful approach to drug delivery. *Drug Discov. Today*, **10**, 1451-1458.

19. Veronese, F.M. & Mero, A. (2008). The impact of PEGylation on biological therapies. *BioDrugs*, **22**, 315-329.

20. Pasut, G. & Veronese, F.M. (2009). PEGylation for improving the effectiveness of therapeutic biomolecules. *Drugs Today (Barc.)*, **45**, 687-695.

21. Mero, A., Clementi, C., Veronese, F.M. & Pasut, G. (2011). Covalent conjugation of poly(ethylene glycol) to proteins and peptides: strategies and methods. *Methods Mol. Biol.*, **751**, 95-129.

22. Sullivan, B.J., Durani, V. & Magliery, T.J. (2011). Triosephosphate Isomerase by Consensus Design: Dramatic Differences in Physical Properties and Activity of Related Variants. *J. Mol. Biol.*, **413**, 195-208.

23. Freitas, Dda. S. & Abrahão-Neto, J. (2010). Biochemical and biophysical characterization of lysozyme modified by PEGylation. *Int. J. Pharm.*, **392**, 111-117.

24. Imoto, T. & Yagishita, K. (1971). A simple activity measurement of lysozyme. *Agric. Biol. Chem.*, **35**, 1154–1156.

25. Lavinder, J.J., Hari, S.B., Sullivan, B.J. & Magliery, T.J. (2009). High-throughput thermal scanning: a general, rapid dye-binding thermal shift screen for protein engineering. *J. Am. Chem. Soc.*, **131**, 3794-3795.

26. Goel, A., Colcher, D., Baranowska-Kortylewicz, J., Augustine, S., Booth, B.J., Pavlinkova, G. & Batra, S.K. (2000). Genetically engineered tetravalent single-chain Fv of the pancarcinoma monoclonal antibody CC49: improved biodistribution and potential for therapeutic application. *Cancer Res.,* **60,** 6964-71.

27. Pavlinkova, G., Beresford, G.W., Booth, B.J.M., Surinder K. Batra, S.K. & Colcher, D. (1999). Pharmacokinetics and Biodistribution of Engineered Single-Chain Antibody Constructs of MAb CC49 in Colon Carcinoma Xenografts. *J. Nucl. Med.*, **40**, 1536-1546.

28. Karlsson, R., Michaelsson, A. & Mattsson, L. (1991). Kinetic analysis of monoclonal antibody-antigen interactions with a new biosensor based analytical system. *J. Immunol. Methods*, **145,** 229-240.

29. Wray, C.J., Lowy, A.M., Matthews, J.B., James, L.E., Mammen, J.M., Choe, K.A., Hanto, D.W. & Ahmad, S.A. (2007). Intraoperative margin re-resection for colorectal liver metastases. *J. Surg. Educ.* **64**, 150-7.